Stress Shielding of the Rotator Cable in the Lateral Rotator Cuff

by

Sean M. Delserro

B.S. in Mechanical Engineering, University of Pittsburgh, 2013

Submitted to the Graduate Faculty of

Swanson School of Engineering in partial fulfillment

of the requirements for the degree of

Master of Science in Mechanical Engineering

University of Pittsburgh

2019

UNIVERSITY OF PITTSBURGH

SWANSON SCHOOL OF ENGINEERING

This thesis was presented

by

Sean M. Delserro

It was defended on

April 3, 2019

and approved by

Mark C. Miller Ph.D., Associate Research Professor, Department of Mechanical Engineering and Materials Science

Christopher C. Schmidt MD, Assistant Research Professor, Department of Orthopaedic Surgery

Qing-Ming Wang Ph.D., Professor, Department of Mechanical Engineering and Materials Science

Thesis Advisor: Patrick Smolinski Ph.D., Associate Professor, Department of Mechanical Engineering and Materials Science

Stress Shielding of the Rotator Cable in the Lateral Rotator Cuff

Sean M. Delserro, M.S.

University of Pittsburgh, 2019

The goal of the project was to test and quantify the biomechanical behavior of the rotator cable and crescent area, as measured by strain and abduction force. The hypothesis was 1) the rotator cable stress shields the crescent area and 2) the rotator cable transmits load during shoulder abduction.

Strain and abduction force were measured for the native, anterior or posterior rotator cable release and anterior and posterior cable release in 10 cadaveric specimens. A computer-controlled shoulder simulator, which applies known loads on the rotator cuff muscles, was developed to measure forces generated at the distal humerus and major principal strain and strain angle in the superior portion of the rotator cuff in cadaveric shoulders at three abduction angles: at 0°, 45° and 90° of scapular plane abduction..

Abduction force significant dropped significantly dropped after single release and full release of the rotator cable at 0° abduction for both the anterior and posterior initial release groups. Significant difference was found in major principal strain in zone 2 of the anterior group at 0° abduction between the native and full release condition. At 30° of abduction significant difference in strain angle was found between intact vs. full release and anterior release vs. full release in the anterior group at zone 16. No other significant differences were found in major principal strain or strain angle.

Although significant differences in major principal strain and strain angle were found, they were few and provided no pattern. We believe this is sufficient evidence to suggest that the rotator cable does not stress shield the lateral crescent region. Releasing the cable insertion sites did significantly decrease the abduction force generated at 0° abduction. Therefore, the rotator cable and crescent region are important structures in initiating shoulder abduction and tears in these regions are biomechanically significant and should be repaired accordingly.

Table of Contents

List of Tables

List of Figures

Preface

First, I would like to thank my advisors for their guidance and support: Dr. Chris Schmidt, Dr. Patrick Smolinski and Dr. Mark Miller. I could not have asked for a better mentor as my time as a graduate student. I would also like to thank the graduate students and orthopedic fellows for their help conducting experiments: Michael Smolinski, Tyler Madonna, Brandon Brown and Dr. Brian Chenoweth. Finally, I would like to thank all my friends and family for their support and encouragement.

1.0 Introduction

1.1 Motivation

This study evaluated the strain in the rotator cuff complex specifically in the lateral tendinous area surrounded by the rotator cable structure where the rotator cuff tendons insert on the humerus. Degenerative rotator cuff tears typically form near the junction of the supraspinatus and infraspinatus, specifically in a region 13 to 17 mm posterior to the biceps tendon. This region also corresponds approximately to the center of the rotator crescent area [1]. Burkhart et al. first described the rotator crescent as a thin, crescent-shaped sheet of rotator cuff comprising of the distal portions of the supraspinatus and infraspinatus insertions. Proximally, the crescent is bounded by a thick bundle of transverse fibers spanning the insertions of the supraspinatus and infraspinatus tendons, termed the rotator cable [2,3]. Burkhart further hypothesized the rotator cable acts as a suspension bridge; stress shielding the crescent area from loads generated from the rotator cuff musculature.

1.2 Goals

The goal of this project was to determine if the rotator cable structure provided any mechanical relief of the lateral tendinous region and thus its implications on tear propagation, superior capsule reconstruction and abduction force. The results could allow surgeons to

understand how rotator cuff tears propagate and the proper repair techniques that can be used to improve surgical outcomes.

2.0 Background

2.1 Anatomic Definitions

The human body can be oriented in many different positions. Therefore, a standard set of terms has been defined to describe anatomical directions and features. Anatomical positions and directions are defined in reference to a standard anatomical position, Figure 1. The standard anatomical position for humans consists of an individual standing with arms hanging at the side, hands (palm) and head are facing forward.

According to the standard anatomical position, the terms anterior and posterior are used to describe the front and back of the body, respectively. Superior and inferior are used to describe the relation to the head of the body. Superior refers to being closer to the head while inferior refers to closer to the feet (or away from the head). Medical and lateral are used to describe an object's relation to the vertical midline of the body. Medial is closer to the midline and lateral is farther away from the midline. Distal and proximal are used to describe location along the extremities. Proximal is closer to the trunk while distal is farther away from the trunk. For example, the shoulder is proximal to the elbow and the wrist is distal to the elbow. Rotation toward the midline and away from the midline are referred to as internal and external rotation, respectively.

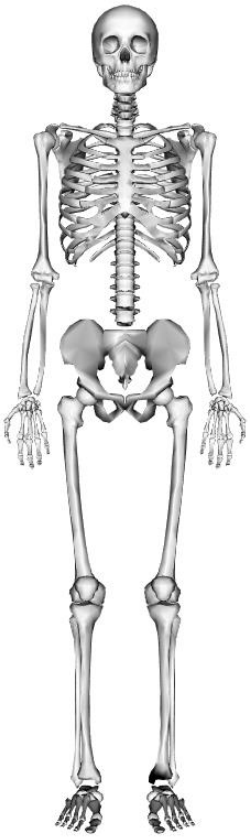

Figure 1. Human skeleton in the standard anatomical position [3]

2.2 Shoulder Anatomy

The anatomical focus of this research is the shoulder, specifically the rotator cuff and rotator cable-crescent complex. The shoulder joint is comprised of two bones: humerus and scapula. The scapula is medial to the humerus and contains the glenoid (socket) to which the proximal end of the humerus (ball) is allowed to articulate; mimicking a ball-and-socket joint. The distal end of the humerus extends to the elbow. As a ball-and-socket joint, the shoulder is able to generate a wide range of movement: abduction/adduction, flexion/extension and internal/external rotation. Shoulder bone anatomy and relevant articulations are shown in Figures 2, 3.

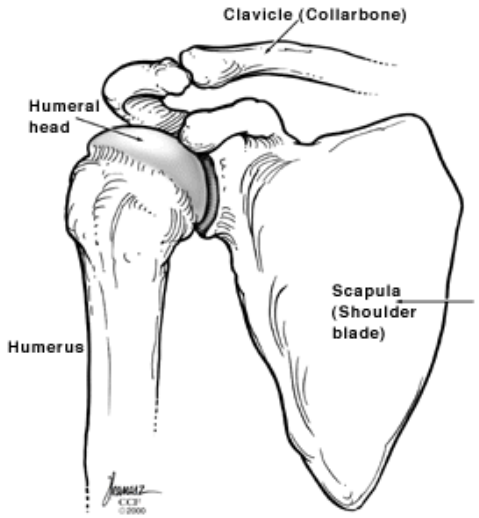

Figure 2. Shoulder Skeletal Anatomy [4]

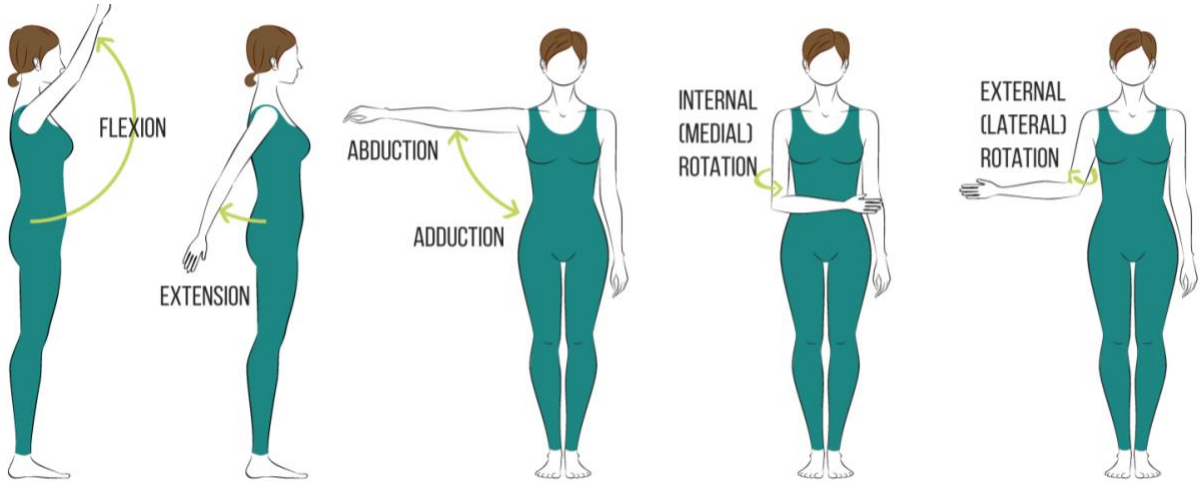

Figure 3. Shoulder Range of Motion (www.sequencewiz.org)

Abduction is the lifting of the upper limb at its side, such that angle between the upper limb and the torso increases. Adduction decreases the angle between the upper limb and the torso. Flexion is defined as raising the upper limb towards the front of the body, while extension is moving the upper limb towards the back of the body. Internal and external rotation describe the rotation of the upper limb about its long axis. Rotation of the upper limb towards the midline, so

that the thumb is pointing medially describes internal rotation. External rotation is the rotation of the upper limb away from the midline, so that the thumb is pointing laterally.

Many muscles are involved in the motion of the shoulder, shown in Figures 4-6. These muscles are necessary for abduction/adduction, flexion/extension and internal/external rotation as well as joint stability. The main muscles involved in abduction are the middle deltoid and supraspinatus. Flexion is achieved through work done by the pectoralis major and anterior deltoid, while extension is achieved by the posterior deltoid, latissimus dorsi and teres major. Internal rotation is produced by the subscapularis, pectoralis major, latissimus dorsi, teres major and anterior deltoid. External rotation is produced by infraspinatus and teres minor. Primary joint stability is maintained through force coupling of the subscapularis, supraspinatus, infraspinatus and teres minor muscles (rotator cuff).

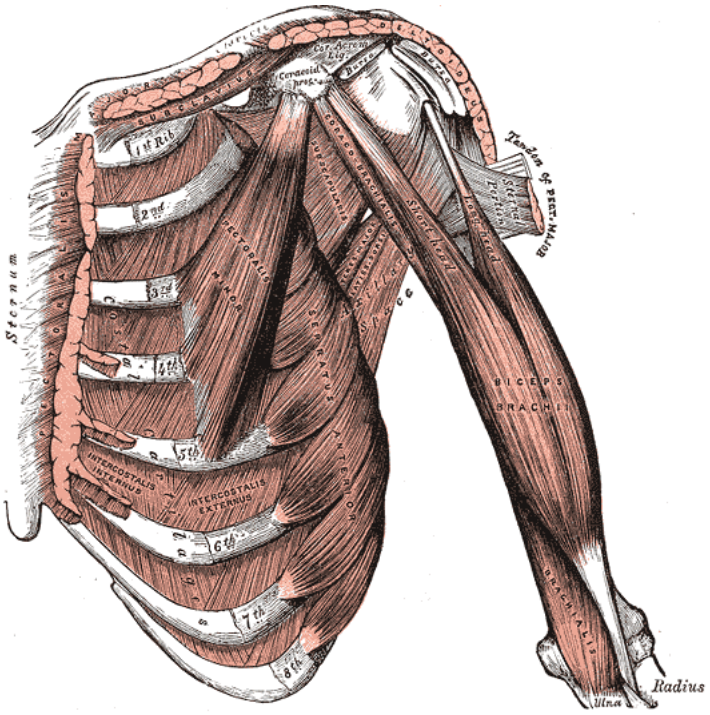

Figure 4. Anterior Shoulder Muscular Anatomy [4]

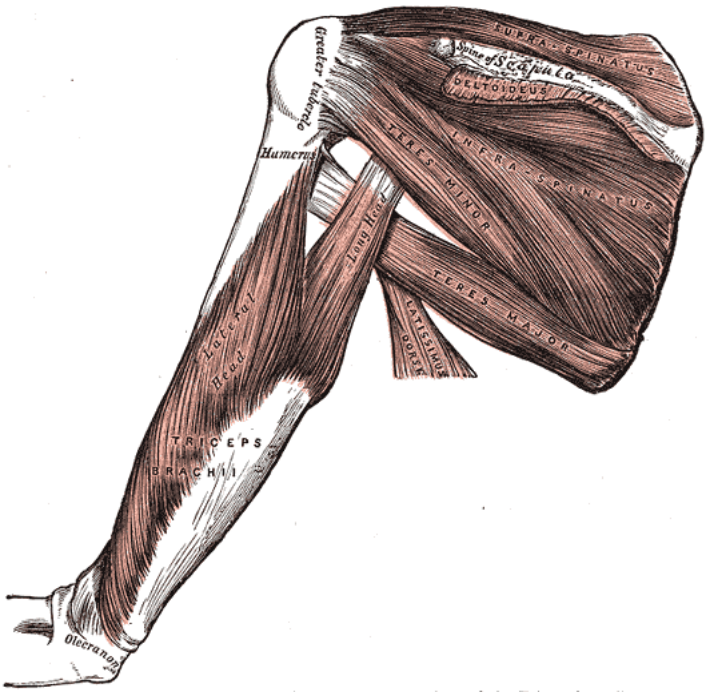

Figure 5. Posterior Shoulder Muscular Anatomy [4]

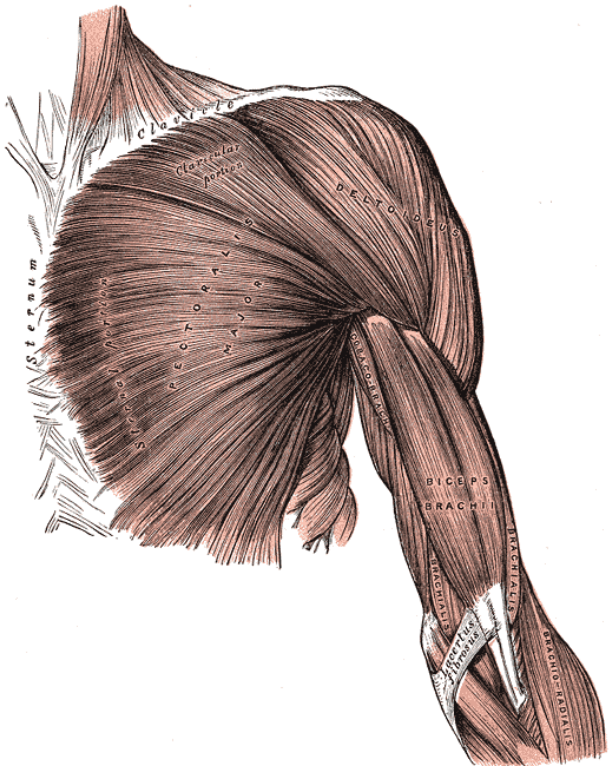

Figure 6. Deltoid Muscle [4]

2.3 Rotator Cuff/Capsule Anatomy

The rotator cuff complex is a group of muscles and tendons that surround the shoulder joint, maintaining shoulder stability and active shoulder movement. Four muscles make up the rotator cuff (spanning from anterior to posterior); the subscapularis, supraspinatus, infraspinatus and teres minor. The subscapularis originates on the subscapular fossa on the anterior surface of the scapula and travels laterally where it inserts into the lesser tuberosity of the humerus and the front of the shoulder joint capsule. The supraspinatus originates at the supraspinatus fossa on the scapula above its spine and travels laterally where it inserts on the greater tuberosity of the humerus at the superior facet. The infraspinatus originates on the infraspinatus fossa of the scapula and travels laterally where it inserts at the posterior aspect of the greater tuberosity of the humerus, and the capsule of the shoulder joint. The teres minor originates on the upper two-thirds of the lateral border of the scapula and travels laterally where it inserts into the inferior facet of the greater tubercle of the humerus and directly below the inferior facet of the greater tubercle of the humerus.

The underlying capsule forms a thin sheath around the shoulder attaching laterally at the neck of the humerus and medially on the glenoid and labrum. The capsule beneath the supraspinatus and infraspinatus tendons is thickened by a strip of fibrous tissue, one centimeter wide, that runs posteriorly in a direction perpendicular to the fibers of the tendons. This strip begins near the coracohumeral ligament insertion and extends to the posterior edge of the infraspinatus tendon [5]. Burkhart et al. termed this band the rotator cable and described its mechanical significance to that of a suspension bridge; shielding the semilunar lateral capsule region, termed the crescent, from stress. Furthermore, Burkhart suggests that tears within the relatively stress-shielded crescent may be biomechanically insignificant [2,3].

2.4 Rotator Cuff/Capsule Injuries

Tears of the rotator cuff are sometimes well-tolerated and do not need surgical treatment. However, in other cases the pain can no longer be tolerated or functional impairment that cannot be treated with conservative therapy results, then surgery may be required. If the tear is large enough to be considered a "massive" cuff tear, surgical treatment may be difficult. These are often called irreparable rotator cuff tears. They are not reparable because of tendon retraction with inelasticity, muscle atrophy, and fatty infiltration [6,7].

Loss of function and pain in the shoulder as a result of rotator cuff injuries occurs due to a disruption in the force balance provided by the rotator cuff musculature and thus instability. Patients with irreparable rotator cuff tears have a defect in the superior capsule, which creates discontinuity of the shoulder capsule in the transverse direction [6,7].

2.5 Strain

Provided a cartesian coordinate system is used, strain can be expressed in terms of its normal x and y components, ϵ_{xx} and ϵ_{yy}, respectively as well as the shear strain, ϵ_{xy}, equations 1-3. Substituting these values into equation 4, we can calculate the principal (maximum and minimum) strains and the principal strain angle, θ_p, from equation 5.

$$\boldsymbol{\epsilon_{xx} = \frac{\partial u_x}{\partial x}} \qquad \textbf{(2-1)}$$

$$\epsilon_{yy} = \frac{\partial u_y}{\partial y} \quad \textbf{(2-2)}$$

$$\epsilon_{xy} = \frac{1}{2}\left(\frac{\partial u_x}{\partial y} + \frac{\partial u_y}{\partial x}\right) \quad \textbf{(2-3)}$$

$$\epsilon_{1,2} = \frac{\epsilon_{xx} + \epsilon_{yy}}{2} + \sqrt{\left(\frac{\epsilon_{xx} - \epsilon_{yy}}{2}\right)^2 + \left(\epsilon_{xy}\right)^2} \quad \textbf{(2-4)}$$

$$tan2\theta_p = \frac{2\epsilon_{xy}}{\epsilon_{xx} - \epsilon_{yy}} \quad \textbf{(2-5)}$$

Stress can also be related strain if material is linear and Young's Modulus, E, is known. Based on equation 6, we can see that stress and strain are directly related.

$$\epsilon = \frac{\sigma}{E} \quad \textbf{(2-6)}$$

As it relates to the rotator cuff and the rotator cable concept, forces are generated in the rotator cuff musculature causing the humerus to pivot about the humeral head in the glenoid, leading to motion of the upper extremity. As the muscles are loaded according to the desired movement, deformation occurs, defined above as strain. Measuring the strain pattern in the rotator

cuff as the muscles are loaded allows the opportunity to test the suspension bridge theory of the rotator cable.

2.6 Previous Strain Work

Early strain measurements used a Hall effect strain transducer (HEST) to measure in vivo displacement behavior and calculate the specimens strain response. Renström et al, used a HEST to measure strain in the anterior cruciate ligament (ACL) during hamstring and quadriceps activity [9]. More recent studies have used a differential variable reluctance transducer (DVRT) to measure strain. Reilly et al, used a DVRT to calculate the strains of the supraspinatus tendon in vitro on both the bursal and articular surfaces [10]. The shoulder joint was disarticulated and only the humeral portion was used for analysis. All soft tissue, except for the supraspinatus, was removed and sutures were tied into the musculotendinous junction of the supraspinatus. Weights were placed at the end of the suture line for uniform loading. The DVRTs were attached to the bursal and articular side of the tendon where any elongation of tissue was subsequently translated to the sliding wire core of the DVRT and strain was calculated. Mazzocca et al performed a similar study investigating the effects of partial-thickness tears and their effects on the supraspinatus tendon [11].

In 2009, Andarawis-Puri published a study investigating the correlation of tendon strain and tear propagation in sheep infraspinatus tendons utilizing a digital image correlation system (DIC) to measure strain [12]. The benefits of the DIC system to measure strain is the use of an optical tracking system and reflective markers which do not interfere with the mechanical dynamics of the specimen of interest. HEST, DVRT and strain gauges all need to be physically

attached to the specimen to measure strain which could alter the mechanical properties of the specimen. The bursal side of the tendon was air-brushed with a fine black paint to create a speckled texture for strain analysis in the DIC.

3.0 Methods

3.1 Overview

The goal of this study was to determine whether the rotator cable strain shields the lateral rotator cuff region of the superior capsule of the shoulder by applying physiological force vectors to the rotator cuff complex and measuring strain and generated abduction force at the distal humerus.

Isometric strain and abduction force were measured in ten cadaveric specimens. The specimens were mounted in a custom designed shoulder simulator, which consisted of five computer controlled linear actuators and a pulley system to apply physiological force vectors. The humerus was abducted and fixed at three positions: 0°, 30° and 60° of glenohumeral abduction relating to 0°, 45° and 90° of scapulothoracic abduction, respectively [8]. Internal and external rotation was fixed at neutral for the purposes of this project. The individual rotator cuff muscles were loaded, and the generated abduction force and strain were measured for the native rotator cuff-capsule complex. The rotator cable's insertion site was then cut anteriorly or posteriorly and retested. The opposing insertion site cut was then made, completely releasing the rotator cable and the final test was performed.

Repeated Measures ANOVA followed by post hoc Bonferroni correction statistical analysis was performed on each zone to determine if releasing the rotator cable had any effect on strain.

3.2 Shoulder Simulator

Support for the shoulder, actuators and pulley system for the application of loads was provided by a custom designed framework Figure 7. The box-shaped framework was designed such that the force applied by the mounted actuators would route physiologically, through the use of the pulley system, to their respective muscles in the cadaveric specimen. 80/20® extruded aluminum, used for its versatility and ease of assembly, made up the majority of the shoulder simulator skeleton. The five actuators were mounted on the rear of the skeleton with their pistons facing upward. Single degree-of-freedom load cells [MLP-100, Transducer Techniques] were screwed to each of the actuator pistons so that the individual actuator forces could be used for feedback control. Eyebolts were screwed into the opposite end of the load cells where 100 lb test line was attached to transmit the actuator loads to their respective rotator cuff muscles.

Figure 7. Shoulder Simulator

Five pulleys were mounted above the actuators to shift the force vectors towards the front of the frame where the specimen is mounted. Another set of custom designed pulleys, Figure 8, were mounted between the specimen and the prior mentioned pulleys which were free to rotate about a joint, allowing natural centering of the test line towards its attachment on the specimen.

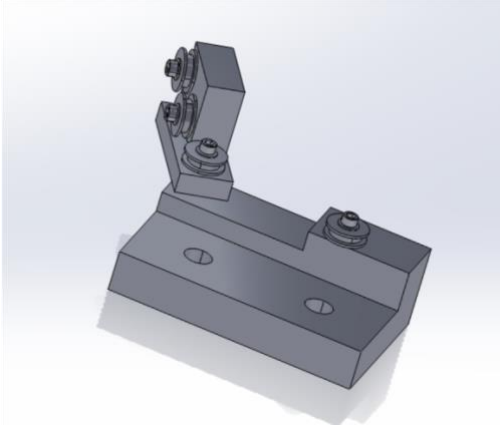

Figure 8. Custom Swivel Pulleys

A custom designed semi-circular arc was placed at the opposite end of the actuators where the distal end of the humerus was fixed. The arc consisted of a ½" acrylic arc sandwiched in between two ¼" steel arcs providing stability from forces that may be generated on the distal arm. The inner diameter of the acrylic arc was greater than that of the steel arcs creating a slot for the distal arm extension to slide along. The glenohumeral joint center was positioned in the center of this arc through a two degree of freedom custom designed drawer system. The semi-circular arc also allowed for adjustment of glenohumeral abduction angle as well as internal-external rotation. For the purposes of this project, the internal-external external rotation was maintained at neutral.

The distal arm extension completed the connection of the distal humerus to the semi-circular arc. A hollow aluminum cylinder encapsulated the potted transected humerus. Radial set screws were used to adjust (both axially and radially) and fix the potted humerus inside the aluminum cylinder. An adapter plate was fabricated to attach the cylinder to a six degree-of-freedom load cell (PY6, Bertec Corporation). It was from this load cell that abduction force and other force data was able to be measured. Continuing distally, the other end of the load cell was attached to perpendicular acrylic plate which glided along the inner diameter and maintained the distal arm extension's position in the slot of the arc.

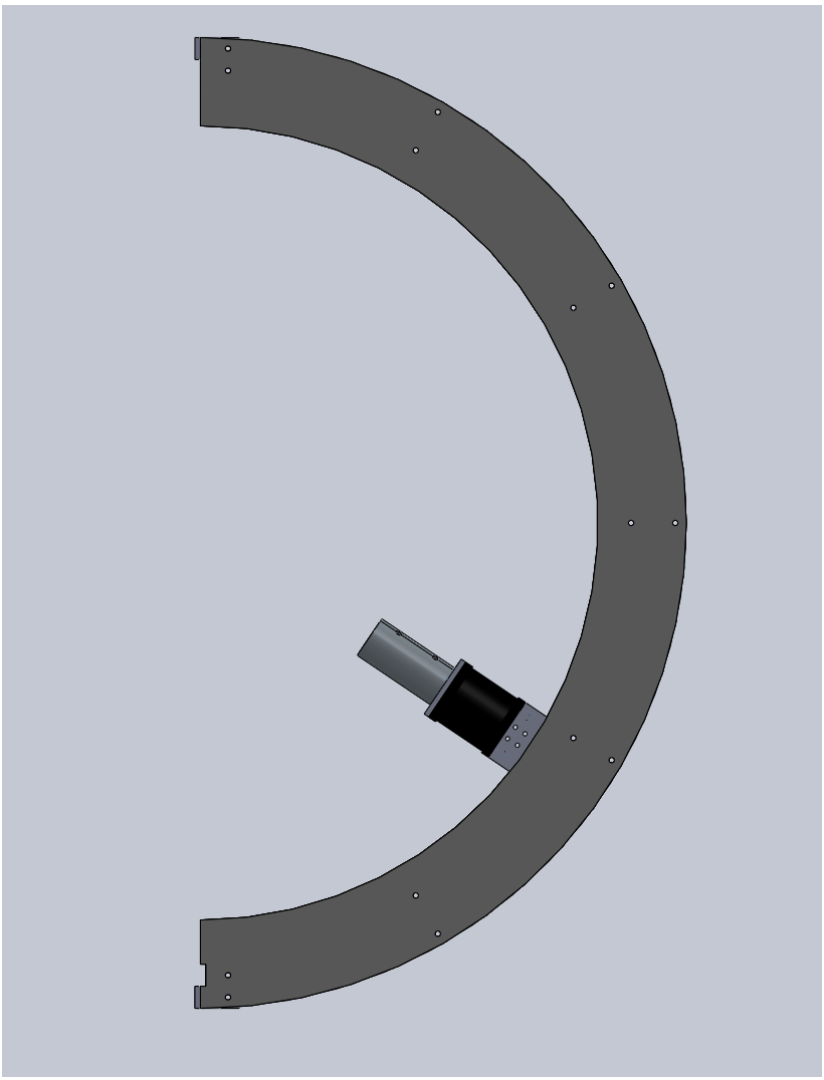

Figure 9. Arc Assembly with Distal Arm Attachment

The scapular portion of the specimen was potted in a five-sided aluminum scapular box. All five sides of the scapular box were able to be disassembled which allowed for reuse of the scapular box between specimens. Holes were drilled into the back side (medial) of the scapular box where the test lines from the actuators were able travel through according to specimen-specific physiological force vectors.

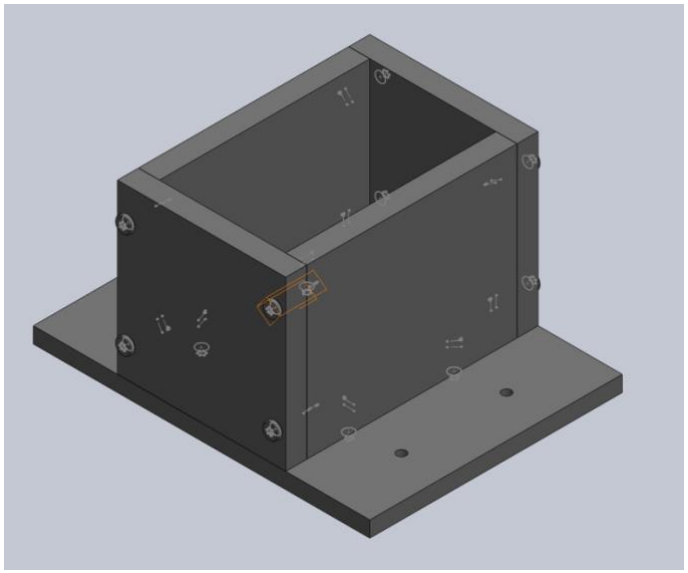

Figure 10. Scapular Box

3.3 Digital Image Correlation

Strain was measured using a Digital Image Correlation (DIC) system (VIC 3D, Correlated Solutions). DIC is an optical tracking system which measures deformation of an object's surface. The system tracks the changes in gray value pattern in small neighborhoods called subsets, indicated by a speckle pattern, during deformation. The VIC 3D system is able to measure strains down to $10\mu\varepsilon$ as well as dynamic events with a frame rate of 5,000,000 frames per second. A two-camera set up was utilized to measure 3-dimensional strain in the rotator cuff (VIC 3D specimen size: 1mm to 50m). The benefits of using a DIC system to measure strain versus HEST, DVRT or strain gauges is discussed in section 2.6.

3.4 Data Acquisition

The outputs of the linear load cells, used to load the rotator cuff muscles, were connected to signal conditioners (LCA-RTC, Transducer Techniques) which fed into the feedback control system for the actuators. The outputs of the signal conditioners were connected to servo drives (Compax3, Parker Hannifin Corporation) for each individual linear actuator. Utilizing a proportional-integral controller (DMC-4080, Galil Motion Control), the error signal between the measured and desired loads was continuously calculated and adjusted the motor velocity and direction accordingly.

The outputs of the 6-DOF load cell, used to measure abduction force and other distal arm forces and moments, were connected to an external digital-to-analog converter and fixed gain analog amplifier (AM6501, Bertec Corporation) and then to a data acquisition board (NI USB-6008, National Instruments) where the signal could be collected and stored in Matlab Software. The outputs of the DIC were collected and analyzed internally through the use of VIC-3D software. The data was then exported into a Matlab format to be further analyzed.

3.5 Cadaveric Specimens

A total of ten upper-extremity cadaveric specimens, average age of 67 $\pm$ 12 years, were used. Each specimen included the full arm from the hand to the scapula. Specimens with a medical history of rheumatoid arthritis or degenerative joint disease were excluded. Prior to the day of testing, each specimen was allowed to thaw 18 hours at room temperature and kept moist with normal saline.

3.6 Cadaveric Specimen Preparation

The humerus was transected at mid shaft and the proximal extremity was isolated. Subcutaneous tissue was removed revealing the deltoid and underlying musculature. The deltoid and soft tissue of the humerus were removed next, and the acromion process was transected to allow for clear observation of the rotator cuff. The rotator cuff muscles were released from their scapular origins and transected slightly proximal to their musculotendinous junctions. A Krackow locking loop stitch, using 2-0 Fiberwire suture (Arthrex, Inc., Naples, FL), was placed into each of the rotator cuff muscles; teres minor, infraspinatus, supraspinatus, subscapularis. The subscapularis was split into two, upper and lower, due to its wide origin on the scapula. The scapula and humerus were cleaned of any loose soft tissue for better adherence to the potting material. Origin sites of the supraspinatus, infraspinatus and upper subscapularis were identified, and eyelet screws were placed mid origin for physiological routing of the sutures.

Epoxy resin was used as the potting material and was mixed and poured into the scapular box and PVC cylinder prior to insertion of scapula and humerus, respectively. Plastic tubing, extending from the top surface of the box and routing physiologically to the rear (medial) end of the box, was used to provide a free pathway for the teres minor and lower subscapularis sutures. The specimen was placed in the scapular box and PVC cylinder after the epoxy was poured and the setup was allowed to harden. Careful consideration was placed on making sure the medial edge of the scapular was parallel with the rear face of the box as well as the medial-lateral line of the specimen was parallel to the side walls of the box. Once hardened, holes were drilled through the rear wall where the teres minor and lower subscapularis sutures could pass through and connect to their respective actuator test line. Infraspinatus, supraspinatus and upper subscapularis were also

connected to their respective actuator test lines and the box was fixed to the shoulder simulator apparatus. pictures

A black ink speckle pattern, Figure 11, was applied to the surface of the rotator cuff for DIC measurement. Care was taken during application to create a unique pattern with small speckles for better accuracy and resolution.

Figure 11. Black Ink Speckle Pattern for DIC Measurement

3.7 Rotator Cable Release

Three cable release conditions were tested in this experiment: intact, anterior or posterior release, and full release (anterior and posterior). The anterior or posterior release conditions were created by an incision between the coracohumeral ligament and supraspinatus tendon (anterior) or between the infraspinatus and teres minor tendons (posterior). The initial release was randomized between specimens. Following completion of the native and anterior or posterior release, an incision was made on the opposite rotator cable attachment, completely releasing the rotator cable from its attachment on the humerus.

3.8 Test Protocol

Prior to each test, the specimen was mounted in the shoulder simulator apparatus and the joint center was aligned with the center of the arc. The distal arm extension was attached to the potted humerus and adjusted so there were no artificial forces applied to the specimen; the distal arm extension was adjusted after each change in abduction angle. The rotator cuff sutures were connected with their respective actuator test lines. The DIC camera system was setup overhead of the specimen with the area between the coracohumeral ligament and teres minor in clear focus for both cameras. The camera system was then calibrated with a calibration plate provided by the manufacturers. If possible, the cameras were not moved until each specimen's testing was complete. If the cameras needed to be adjusted, the system was recalibrated.

Starting at 0° abduction for the native condition, the determined physiologic forces were entered into the control system and the actuators were jogged in to increase the preload to 5 N on

each of the rotator cuff muscles. Data acquisition programs were started. Loads were subsequently applied via a ramp profile until the desired load profile had been achieved. Once the load profile was achieved, loads were held constant for approximately 10 seconds to remove any viscoelastic bias inherent in muscle loading. The same loads were applied to each specimen at each abduction angle for each condition. The data acquisition was stopped, and the actuators were returned to their starting position. The humerus was adjusted to 30° glenohumeral abduction (45° humeral-thoracic abduction) [8] and the distal arm extension was adjusted accordingly. The data acquisition and loading procedure was repeated at 30° glenohumeral abduction and 60° glenohumeral abduction (90° humeral-thoracic abduction).

After test completion of the native condition, a random number generator was used to determine whether the specimen would receive an anterior or posterior rotator cable release. Testing was cycled through the three abduction angles under the given anterior or posterior rotator cable release. Finally, the rotator cable was fully released, and testing was again cycled through the three abduction angles. This completed testing for the specimen.

3.9 Identifying Region of Interest

The DIC software required the selection of a region of interest inside of which the software was to analyze the strain pattern. The region of interest (ROI) was unique to each combination of specimen, abduction angle and release condition. The ROI was selected to be the area on the surface of the superior rotator cuff containing the speckle pattern, rotator cable and crescent, Figure 12. From lateral to medial, this region was consistently defined as the area from the tendinous

insertion of the rotator cuff musculature to the musculotendinous junction. From anterior to posterior, this region was consistently defined as the area from the anterior attachment of the rotator cable (anterior border supraspinatus tendon) to the posterior attachment of the rotator cable (posterior border of the infraspinatus tendon).

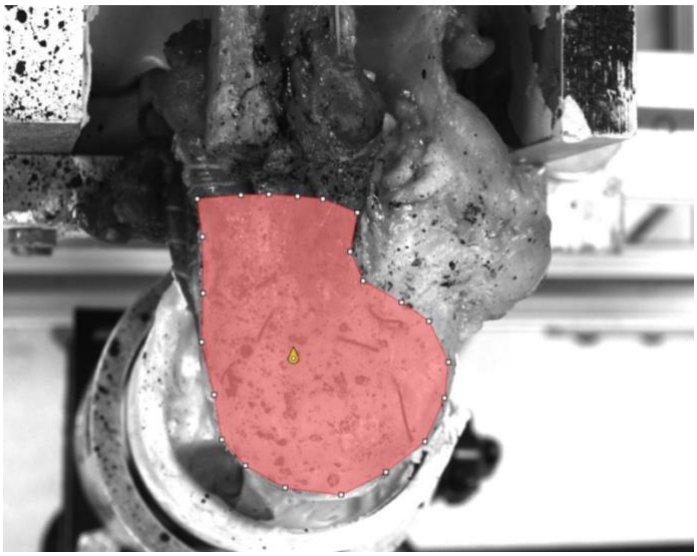

Figure 12. Selection of Region of Interest for DIC data processing

3.10 Data Analysis

Abduction force data was separated into two groups; anterior release first and posterior release first groups. The anterior release group consisted of the 5 specimens which received the anterior release cut first and vice versa for the posterior group. For each group, abduction force was averaged across each rotator cable condition at each abduction angle and compared using a paired student's t-test.

The DIC provides a variety of output data including major/minor principal strains, principal strain angle, strains along x and y coordinate axes, shear strain, strain rate and displacement to name a few. Due to the complex loading pattern of the rotator cuff and the lack of prior biomechanical data in the literature, the major principal strain (E1) and strain angle was analyzed. The DIC software provided a color spectrum plot of the strain data, Figure 13, which was sufficient for visual inspection, however, it was difficult to analyze quantitatively. The data was also organized in a matrix format, with each data point in the matrix correlating to a specific pixel in the image taken by the DIC camera system. This proved to be very useful as it provided spatial orientation of the strain data on the rotator cuff. However, the data sets for each test condition and abduction angle were very large and cumbersome to analyze, Figure 14. A Matlab script was developed to "coarsen" or average the data sets into a 4 x 5 matrix. The data was separated into two groups; anterior release group and posterior release group. The magnitude and direction of each of the data sets were plotted in Matlab (Appendix A).

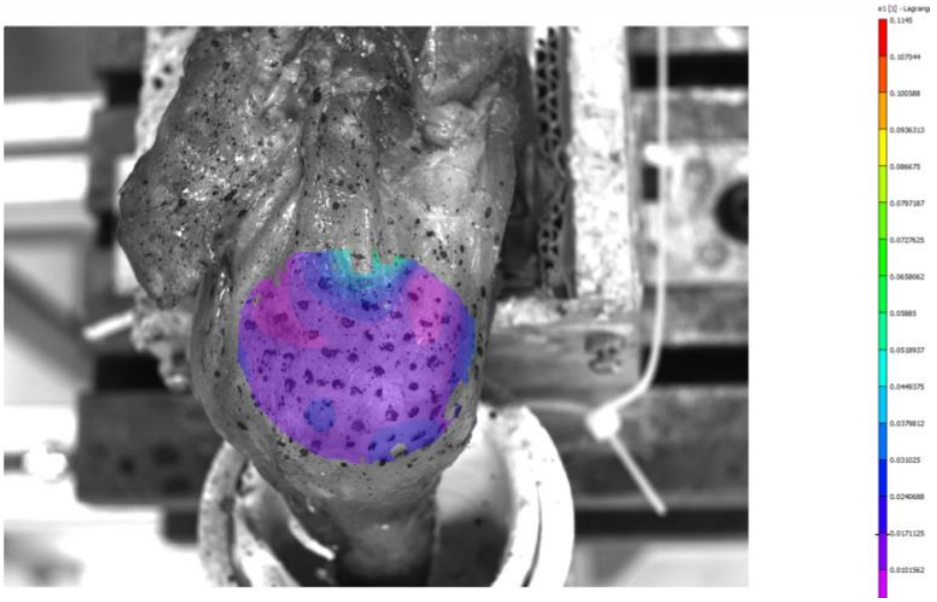

Figure 13. Typical DIC Color Spectrum E1 Strain Plot

The 4 x 5 matrix was separated into 20 “zones”, Figures 15 - 16, corresponding to each of the 20 scalar components of the matrix. Each zone contained 5 values; one for each of the specimens in the group at that specific zone and rotator cuff state (intact, single release, full release). Simply, each zone contains the major principal strain and strain angle values at a specific region on the rotator cuff for the specimens in that group for a given rotator cuff state.

Once the data was separated into distinct zones a vector plot was used to plot the data. The benefits of a utilizing a vector plot was the ability to observe the magnitude and direction of the principal strains, as both magnitude and direction were inputs to the plot function. Statistical analysis was performed by zone using a one-factor repeated measures analysis of variance (ANOVA) with cable state as the factor, followed by post hoc analysis using a Bonferonni correction with statistical significance at $p<0.05$ (SPSS v25, SPSS Inc.).

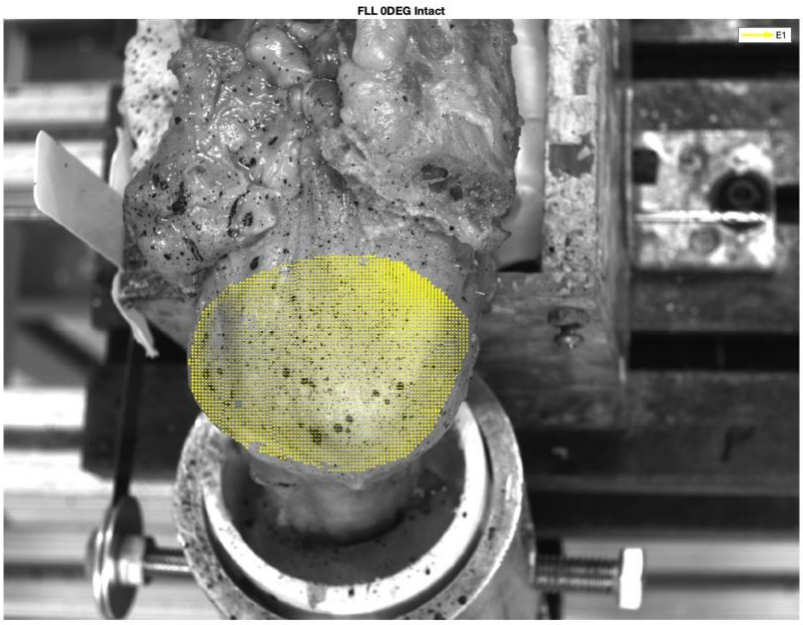

Figure 14. Typical Specimen Strain Vector Plot Before Averaging

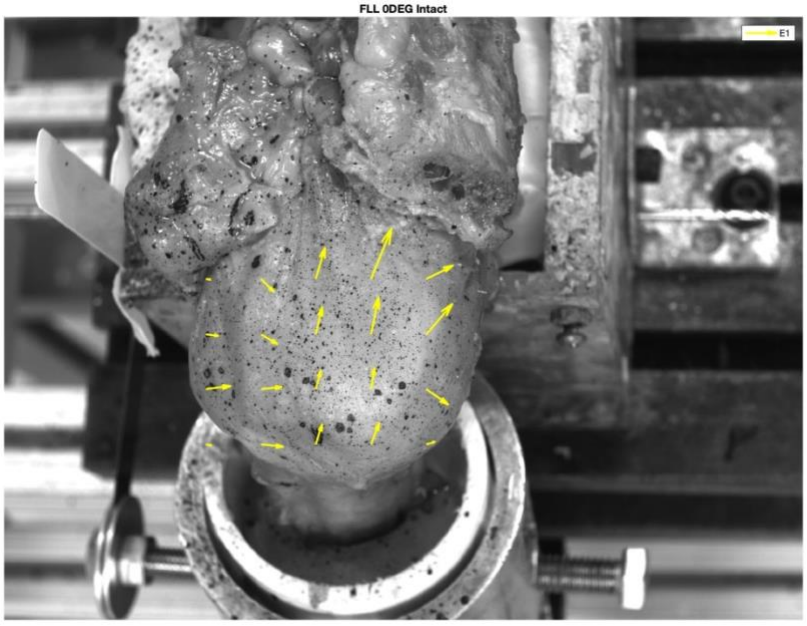

Figure 15. Typical Specimen Strain Vector Plot After Averaging

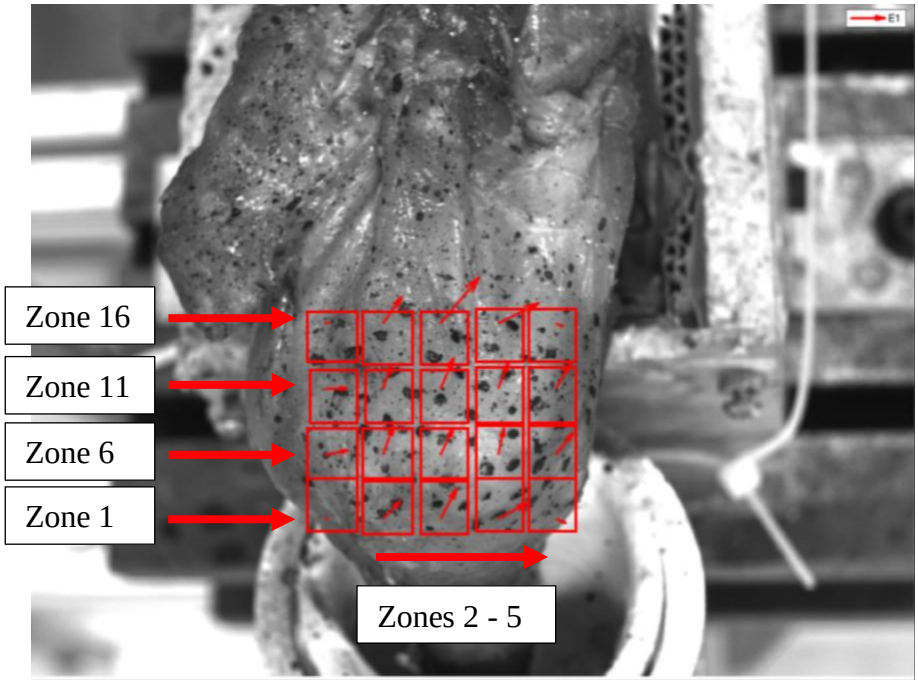

Figure 16. Zone Mapping

4.0 Results

4.1 Abduction Force Results

Abduction force results are shown in Figure 16, Table 1 and Table 2. After the rotator cable was released anteriorly the abduction force decreased significantly in 0° of abduction. The same result significant difference was found for the posterior group at 0° of abduction. Significant difference was found between the intact and full release cable conditions at 0° abduction for the anterior group. Significant difference was also found between the intact and full release cable conditions for the posterior group.

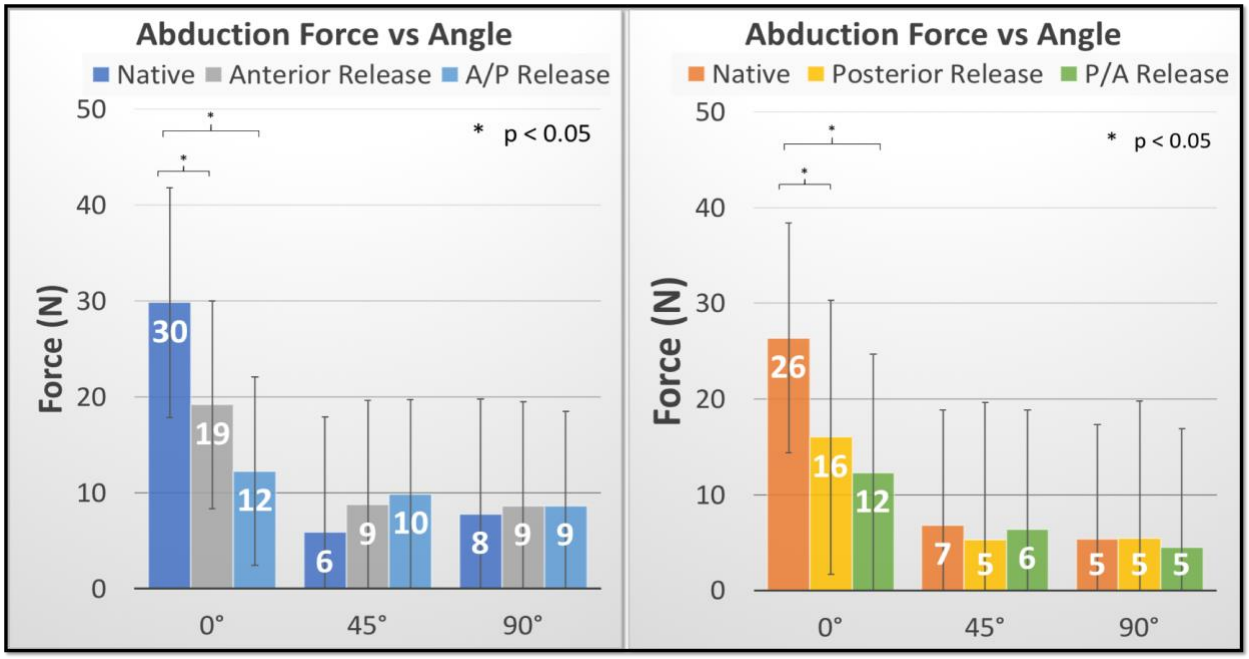

Figure 17. Abduction Force Results vs Abduction Angle (Left - Anterior Group, Right - Posterior Group)

Table 1. Average Abduction Force vs. Abduction Angle (Anterior Group, *, p<0.05)**

Abduction Angle	Intact (N)	Anterior Release (N)	Full Release (N)
0°	29.83 ± 23.47*, **	19.17 ± 10.86*	12.26 ± 9.85**
45°	5.88 ± 4.32	8.76 ± 2.36	9.85 ± 1.65
90°	7.80 ± 3.14	8.63 ± 2.10	8.62 ± 3.88

Table 2. Average Abduction Force vs. Abduction Angle (Posterior Group, *, p<0.05)**

Abduction Angle	Intact (N)	Posterior Release (N)	Full Release (N)
0°	26.37 ± 16.04*,**	16.01 ± 14.32*	12.29 ± 12.43**
45°	6.83 ± 6.64	5.32 ± 6.09	6.40 ± 8.97
90°	5.37 ± 5.49	5.47 ± 4.71	4.50 ± 4.10

4.2 Strain Results

Tables 3 – 14 (Appendix B) give the results of the major principal strain and strain angle for both the anterior and posterior groups. The repeated measures ANOVA showed significant difference in major principle strain magnitude in the anterior group in zone 2 between the intact cable condition and the full release cable condition for 0 degrees of abduction. No other significant differences were found in major principle strain magnitude. At 45 degrees of abduction significant difference in strain angle was found between intact vs. full release and anterior release vs. full release in the anterior group at zone 16. No other significant differences were found in stain angle.

Further statistical analysis was performed on two specific zones; zones 18 and 19 due to their anatomic proximity to the center of the crescent region. Based on the lack of evidence in anterior or posterior cable release having an effect on strain from the repeated measures ANOVA analysis, the anterior and posterior groups were combined, and the intact condition and full release conditions were compared for zones 18 and 19 using a paired t-test ($p = 0.05$). No significant differences were found between conditions in these regions, Figures 18-20 & Tables 15-20 in Appendix B.

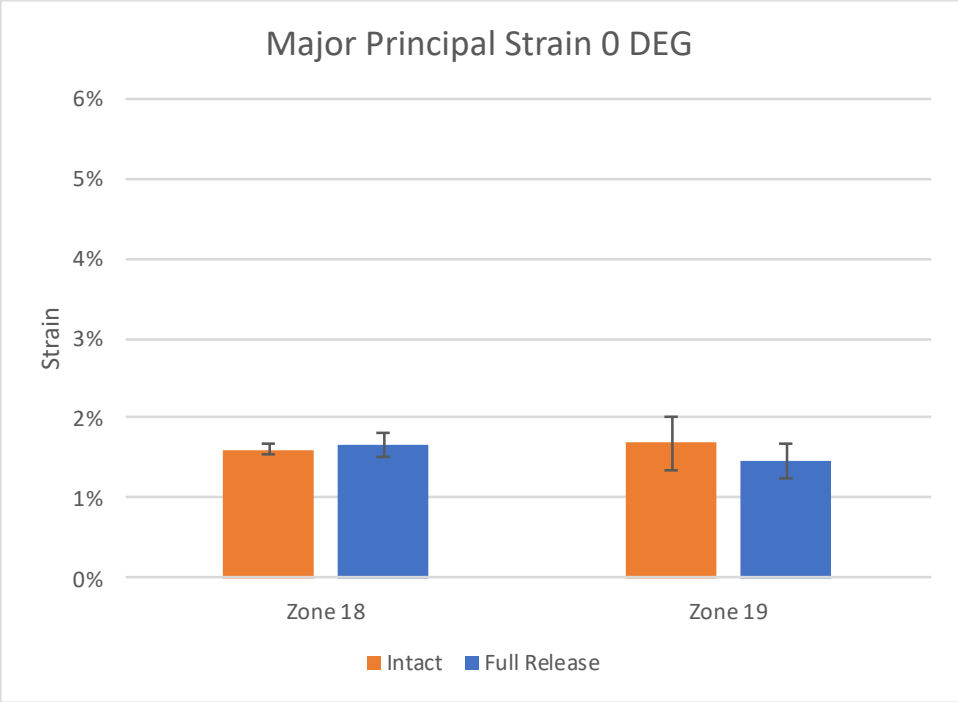

Figure 18. Major Principal Strain Intact vs. Full Release, 0° Abduction , Combined Group, Zones 18 & 19

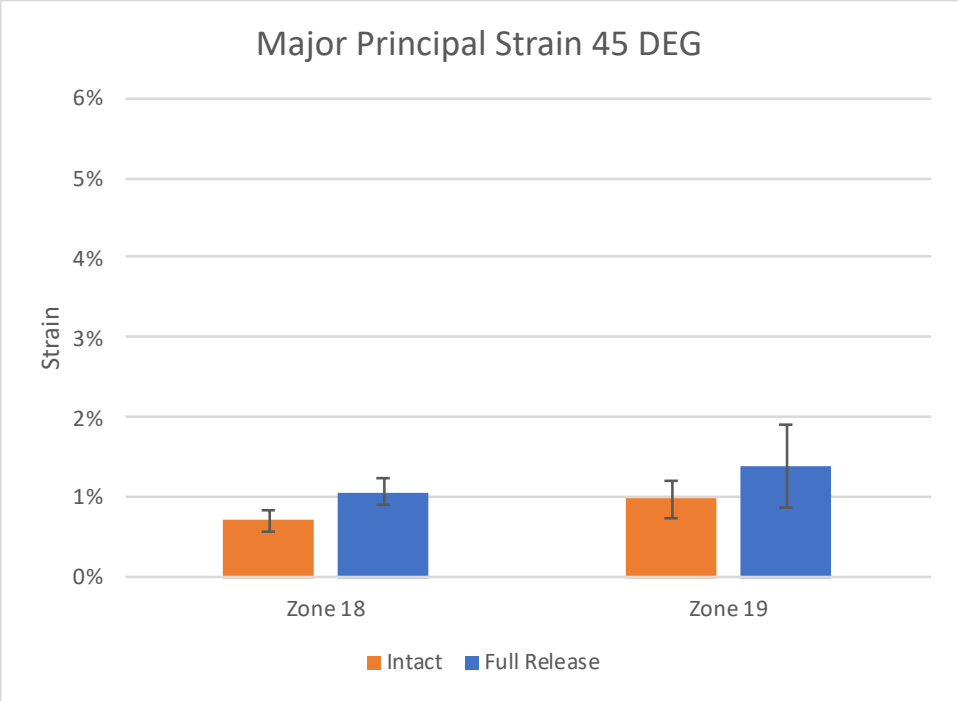

Figure 19. Major Principal Strain Intact vs. Full Release, 45° Abduction, Combined Group, Zones 18 & 19

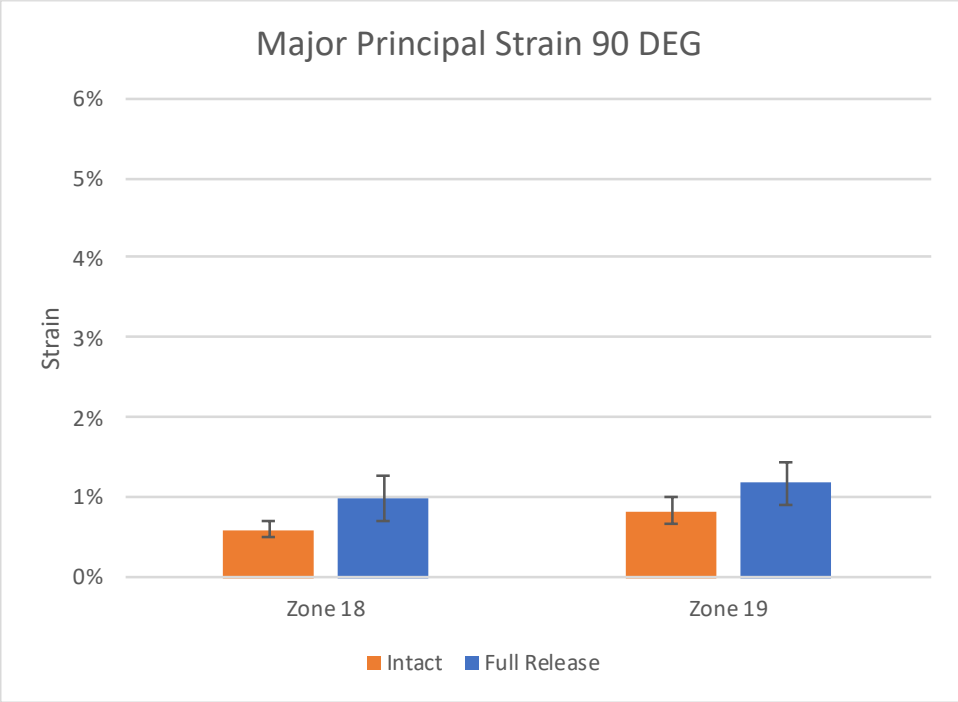

Figure 20. Major Principal Strain Intact vs. Full Release, 90° Abduction, Combined Group, Zones 18 & 19

5.0 Discussion

Burkhart et al. described the rotator cable as a stress shielder to the lateral crescent region which it surrounds; meaning that relatively little force or stress is transmitted to the crescent region as the rotator cuff loads the humerus. Theoretically as force is applied by the rotator cuff musculature, specifically the supraspinatus and infraspinatus, to the humerus, the rotator cable would divert the force transmission circumferentially around the crescent and through the transverse bands of the rotator cable to its insertion sites anteriorly and posteriorly. Therefore, releasing the cable from its insertion sites on the humerus should allow free transmission of force through the cable into the crescent. Stress is directly proportional to force assuming a constant cross-sectional area; thus, as force increases so would stress. Furthermore, strain is directly proportional to stress, assuming constant material properties, and would also increase as stress increases.

Based on our results, we saw relatively no change in major principle strain magnitude or angle upon release of the rotator cable. Significant difference was found in major principle strain magnitude at zone 2 between the intact and full release cable condition for the anterior group, however, no other significant differences were found in major principal strain magnitude. Similarly, significant difference was found in strain angle at zone 16 between the intact and full release, and anterior release and full release cable conditions for the anterior group but no other significant differences were found in strain angle. It is somewhat interesting that the significant differences found were contained in the anterior group only, however, we believe these significant differences to be false positives resulting from high number of comparisons. They are inconsistent and no pattern or conclusion can be interpreted from them. This conclusion was further supported

by our analysis of zones 18 and 19 of the combined groups, where no statistical difference was found between the intact and full release conditions. Therefore, we believe, collectively, this is sufficient evidence to suggest that the rotator cable does not stress shield the lateral crescent region.

We did find releasing the anterior insertion of the rotator cable significantly drops abduction force 37%, followed by full release of both insertions decreases abduction force 60% in 0° of abduction. Similarly, releasing the posterior insertion significantly lowers abduction force by 38% and full release by 54% in 0° of abduction. Greater degrees of abduction showed no significant change in abduction force. These findings indicate the CHL and fibrous band between the infraspinatus and teres minor play an important role in initiating shoulder abduction, but once shoulder elevation is reached the rotator cuff contains enough interconnectivity to center the humerus without lessening native force transmission.

6.0 Conclusion and Future Work

6.1 Conclusions

This biomechanical study suggests that the rotator cable structure does not stress shield the lateral crescent region contrary to prior belief. Furthermore, the rotator cable and crescent area are important structures in initiating shoulder abduction. Therefore, tears in the rotator cable and crescent region are biomechanically significant and should be repaired accordingly.

6.2 Future Work

Due to uncertainty in the precise location of the rotator cable, a new ongoing experiment was designed to verify the locations of important anatomical structures in the rotator cuff complex. During the specimen preparation phase, the inferior capsule is opened to reveal the joint cavity. The humeral head is transected just medial to the rotator cuff insertion sites and the rotator cable is now visible. Suture was loosely passed through and around the full thickness of soft tissue on the medial (outer) and lateral (inner) perimeter of the rotator cable such that rotator cable area is now visible from the bursal side of the specimen.

We have learned that the medial (outer) perimeter of the rotator cable repeatedly is located on or near the musculotendinous junction. Thus, to properly compare strain in the inner and outer portions of the cable, the same material must be used. This was achieved by shaving off the thin muscle exterior of the supraspinatus and infraspinatus muscles just outside the rotator cable

perimeter to reveal the underlying tendons, allowing us to measure strain in the in the outer tendinous regions of the supraspinatus and infraspinatus and the inner crescent tendinous region.

This study is currently ongoing, and we hope to gain more insight into the biomechanical significance of the rotator cable and its relationship to the surrounding rotator cuff complex.

Appendix A Strain Analysis Matlab Code

A.1 Main Data Analysis Code

```
%% Specimen Picture with Quiver overlay
% Written by Sean Delserro
% Graduate Research Assistant
% Shoulder and Elbow Mechanics Laboratory
% May 3, 2018

close all; clc; clear all;

newrows = 4;
newcols = 5;

%%%%%%% A GROUP %%%%%%%%%%

%% DEL
% DEL 0 DEG Intact
DEL00 = load('DE12042792L Strain Data/DE12042792L-0091 OG 0DEG.mat');
DEL00x = dataCoarsen(newrows,newcols,DEL00.x);
DEL00y = dataCoarsen(newrows,newcols,DEL00.y);
DEL00y = DEL00y-80;
DEL00e1 = dataCoarsen(newrows,newcols,DEL00.e1);
DEL00e2 = dataCoarsen(newrows,newcols,DEL00.e2);
DEL00gamma = dataCoarsen(newrows,newcols,DEL00.gamma);
DEL00e1x = DEL00e1.*cos(DEL00gamma);
DEL00e1y = DEL00e1.*sin(DEL00gamma);
DEL00Pic = imread('DE12042792L Strain Data/DE12042792L-0091_0 OG 0DEG.tif');


% DEL 0 DEG A Cut
DEL10 = load('DE12042792L Strain Data/DE12042792L-0273 ACut 0DEG.mat');
DEL10x = dataCoarsen(newrows,newcols,DEL10.x);
DEL10y = dataCoarsen(newrows,newcols,DEL10.y);
DEL10y = DEL10y-80;
DEL10e1 = dataCoarsen(newrows,newcols,DEL10.e1);
DEL10e2 = dataCoarsen(newrows,newcols,DEL10.e2);
DEL10gamma = dataCoarsen(newrows,newcols,DEL10.gamma);
DEL10e1x = DEL10e1.*cos(DEL10gamma);
DEL10e1y = DEL10e1.*sin(DEL10gamma);
DEL10Pic = imread('DE12042792L Strain Data/DE12042792L-0273_0 ACut
0DEG.tif');


% DEL 0 DEG AP Cut
DEL30 = load('DE12042792L Strain Data/DE12042792L-0392 APCut 0DEG.mat');
DEL30x = dataCoarsen(newrows,newcols,DEL30.x);
```

```
DEL30y = dataCoarsen(newrows,newcols,DEL30.y);
DEL30y = DEL30y-80;
DEL30e1 = dataCoarsen(newrows,newcols,DEL30.e1);
DEL30e2 = dataCoarsen(newrows,newcols,DEL30.e2);
DEL30gamma = dataCoarsen(newrows,newcols,DEL30.gamma);
DEL30e1x = DEL30e1.*cos(DEL30gamma);
DEL30e1y = DEL30e1.*sin(DEL30gamma);
DEL30Pic = imread('DE12042792L Strain Data/DE12042792L-0392_0 APCut
0DEG.tif');

%% LAL
% LAL 0 DEG Intact
LAL00 = load('LA12102249L Strain Data/LA12102249L-0057_0 OG 0DEG.mat');
LAL00x = dataCoarsen(newrows,newcols,LAL00.x);
LAL00y = dataCoarsen(newrows,newcols,LAL00.y);
LAL00y = LAL00y-80;
LAL00e1 = dataCoarsen(newrows,newcols,LAL00.e1);
LAL00e2 = dataCoarsen(newrows,newcols,LAL00.e2);
LAL00gamma = dataCoarsen(newrows,newcols,LAL00.gamma);
LAL00e1x = LAL00e1.*cos(LAL00gamma);
LAL00e1y = LAL00e1.*sin(LAL00gamma);
LAL00Pic = imread('LA12102249L Strain Data/LA12102249L-0057_0.tif');

% LAL 0 DEG A Cut
LAL10 = load('LA12102249L Strain Data/LA12102249L-0356_0 ACut 0DEG.mat');
LAL10x = dataCoarsen(newrows,newcols,LAL10.x);
LAL10y = dataCoarsen(newrows,newcols,LAL10.y);
LAL10y = LAL10y-80;
LAL10e1 = dataCoarsen(newrows,newcols,LAL10.e1);
LAL10e2 = dataCoarsen(newrows,newcols,LAL10.e2);
LAL10gamma = dataCoarsen(newrows,newcols,LAL10.gamma);
LAL10e1x = LAL10e1.*cos(LAL10gamma);
LAL10e1y = LAL10e1.*sin(LAL10gamma);
LAL10Pic = imread('LA12102249L Strain Data/LA12102249L-0356_0.tif');

% LAL 0 DEG AP Cut
LAL30 = load('LA12102249L Strain Data/LA12102249L-0602_0 APCut 0DEG.mat');
LAL30x = dataCoarsen(newrows,newcols,LAL30.x);
LAL30y = dataCoarsen(newrows,newcols,LAL30.y);
LAL30y = LAL30y-80;
LAL30e1 = dataCoarsen(newrows,newcols,LAL30.e1);
LAL30e2 = dataCoarsen(newrows,newcols,LAL30.e2);
LAL30gamma = dataCoarsen(newrows,newcols,LAL30.gamma);
LAL30e1x = LAL30e1.*cos(LAL30gamma);
LAL30e1y = LAL30e1.*sin(LAL30gamma);
LAL30Pic = imread('LA12102249L Strain Data/LA12102249L-0602_0.tif');

%% LAR
% LAR 0 DEG Intact
LAR00 = load('LA12102249R Strain Data/LA12102249R-0407_0 OG 0DEG.mat');
LAR00x = fliplr(dataCoarsen(newrows,newcols,LAR00.x));
LAR00y = fliplr(dataCoarsen(newrows,newcols,LAR00.y));
LAR00e1 = fliplr(dataCoarsen(newrows,newcols,LAR00.e1));
LAR00e2 = fliplr(dataCoarsen(newrows,newcols,LAR00.e2));
LAR00gamma = fliplr(dataCoarsen(newrows,newcols,LAR00.gamma));
LAR00e1x = LAR00e1.*cos(LAR00gamma);
```

```
LAR00e1y = LAR00e1.*sin(LAR00gamma);
LAR00Pic = imread('LA12102249R Strain Data/LA12102249R-0407_0.tif');

% LAR 0 DEG A Cut
LAR10 = load('LA12102249R Strain Data/LA12102249R-0721_0 ACut 0DEG.mat');
LAR10x = dataCoarsen(newrows,newcols,LAR10.x);
LAR10y = dataCoarsen(newrows,newcols,LAR10.y);
LAR10e1 = dataCoarsen(newrows,newcols,LAR10.e1);
LAR10e2 = dataCoarsen(newrows,newcols,LAR10.e2);
LAR10gamma = dataCoarsen(newrows,newcols,LAR10.gamma);
LAR10e1x = LAR10e1.*cos(LAR10gamma);
LAR10e1y = LAR10e1.*sin(LAR10gamma);
LAR10Pic = imread('LA12102249R Strain Data/LA12102249R-0721_0.tif');

% LAR 0 DEG AP Cut
LAR30 = load('LA12102249R Strain Data/LA12102249R-0957_0 APCut 0DEG.mat');
LAR30x = dataCoarsen(newrows,newcols,LAR30.x);
LAR30y = dataCoarsen(newrows,newcols,LAR30.y);
LAR30y = LAR30y-80;
LAR30e1 = dataCoarsen(newrows,newcols,LAR30.e1);
LAR30e2 = dataCoarsen(newrows,newcols,LAR30.e2);
LAR30gamma = dataCoarsen(newrows,newcols,LAR30.gamma);
LAR30e1x = LAR30e1.*cos(LAR30gamma);
LAR30e1y = LAR30e1.*sin(LAR30gamma);
LAR30Pic = imread('LA12102249R Strain Data/LA12102249R-0957_0.tif');

%% MDR
% MDR 0 DEG Intact
MDR00 = load('MD12101222R Strain Data/MD1210222R-0132_0 OG 0DEG.mat');
MDR00x = dataCoarsen(newrows,newcols,MDR00.x);
MDR00y = dataCoarsen(newrows,newcols,MDR00.y);
MDR00y = MDR00y-80;
MDR00e1 = dataCoarsen(newrows,newcols,MDR00.e1);
MDR00e2 = dataCoarsen(newrows,newcols,MDR00.e2);
MDR00gamma = dataCoarsen(newrows,newcols,MDR00.gamma);
MDR00e1x = MDR00e1.*cos(MDR00gamma);
MDR00Pic = imread('MD12101222R Strain Data/MD1210222R-0132_0.tif');

% MDR 0 DEG A Cut
MDR10 = load('MD12101222R Strain Data/MD1210222R-0279_0 ACut 0DEG.mat');
MDR10x = dataCoarsen(newrows,newcols,MDR10.x);
MDR10y = dataCoarsen(newrows,newcols,MDR10.y);
MDR10y = MDR10y-80;
MDR10e1 = dataCoarsen(newrows,newcols,MDR10.e1);
MDR10e2 = dataCoarsen(newrows,newcols,MDR10.e2);
MDR10gamma = dataCoarsen(newrows,newcols,MDR10.gamma);
MDR10e1x = MDR10e1.*cos(MDR10gamma);
MDR10e1y = MDR10e1.*sin(MDR10gamma);
MDR10Pic = imread('MD12101222R Strain Data/MD1210222R-0279_0.tif');

% MDR 0 DEG AP Cut
MDR30 = load('MD12101222R Strain Data/MD1210222R-0413_0 APCut 0DEG.mat');
MDR30x = dataCoarsen(newrows,newcols,MDR30.x);
MDR30y = dataCoarsen(newrows,newcols,MDR30.y);
MDR30y = MDR30y-80;
MDR30e1 = dataCoarsen(newrows,newcols,MDR30.e1);
```

```
MDR30e2 = dataCoarsen(newrows,newcols,MDR30.e2);
MDR30gamma = dataCoarsen(newrows,newcols,MDR30.gamma);
MDR30e1x = MDR30e1.*cos(MDR30gamma);
MDR30e1y = MDR30e1.*sin(MDR30gamma);
MDR30Pic = imread('MD12101222R Strain Data/MD1210222R-0413_0.tif');

%% NCL
% 0 DEG Intact
NCL00 = load('NC12081860L Strain Data/NC12081860L-0252_0 OG 0DEG.mat');
NCL00x = dataCoarsen(newrows,newcols,NCL00.x);
NCL00y = dataCoarsen(newrows,newcols,NCL00.y);
NCL00y = NCL00y-80;
NCL00e1 = dataCoarsen(newrows,newcols,NCL00.e1);
NCL00e2 = dataCoarsen(newrows,newcols,NCL00.e2);
NCL00gamma = dataCoarsen(newrows,newcols,NCL00.gamma);
NCL00e1x = NCL00e1.*cos(NCL00gamma);
NCL00e1y = NCL00e1.*sin(NCL00gamma);
NCL00Pic = imread('NC12081860L Strain Data/NC12081860L-0252_0.tif');

% 0 DEG A Cut
NCL10 = load('NC12081860L Strain Data/NC12081860L-0365_0 ACut 0DEG.mat');
NCL10x = dataCoarsen(newrows,newcols,NCL10.x);
NCL10y = dataCoarsen(newrows,newcols,NCL10.y);
NCL10y = NCL10y-80;
NCL10e1 = dataCoarsen(newrows,newcols,NCL10.e1);
NCL10e2 = dataCoarsen(newrows,newcols,NCL10.e2);
NCL10gamma = dataCoarsen(newrows,newcols,NCL10.gamma);
NCL10e1x = NCL10e1.*cos(NCL10gamma);
NCL10e1y = NCL10e1.*sin(NCL10gamma);
NCL10Pic = imread('NC12081860L Strain Data/NC12081860L-0365_0.tif');

%0 DEG AP Cut
NCL30 = load('NC12081860L Strain Data/NC12081860L-0527_0 APCut 0DEG.mat');
NCL30x = dataCoarsen(newrows,newcols,NCL30.x);
NCL30y = dataCoarsen(newrows,newcols,NCL30.y);
NCL30y = NCL30y-80;
NCL30e1 = dataCoarsen(newrows,newcols,NCL30.e1);
NCL30e2 = dataCoarsen(newrows,newcols,NCL30.e2);
NCL30gamma = dataCoarsen(newrows,newcols,NCL30.gamma);
NCL30e1x = NCL30e1.*cos(NCL30gamma);
NCL30e1y = NCL30e1.*sin(NCL30gamma);
NCL30Pic = imread('NC12081860L Strain Data/NC12081860L-0527_0.tif');

%%%%%%% P GROUP %%%%%%%%%%

%% FLL
% 0 DEG Intact
FLL00 = load('FL12110306L Strain/FL12110306L-0063_0 OG 0DEG.mat');
FLL00x = dataCoarsen(newrows,newcols,FLL00.x);
FLL00y = dataCoarsen(newrows,newcols,FLL00.y);
FLL00y = FLL00y-100;
FLL00e1 = dataCoarsen(newrows,newcols,FLL00.e1);
FLL00e2 = dataCoarsen(newrows,newcols,FLL00.e2);
FLL00gamma = dataCoarsen(newrows,newcols,FLL00.gamma);
FLL00e1x = FLL00e1.*cos(FLL00gamma);
FLL00e1y = FLL00e1.*sin(FLL00gamma);
```

```
FLL00Pic = imread('FL12110306L Strain/FL12110306L-0063_0.tif');

% 0 DEG P Cut
FLL20 = load('FL12110306L Strain/FL12110306L-0243_0 PCut 0DEG.mat');
FLL20x = dataCoarsen(newrows,newcols,FLL20.x);
FLL20y = dataCoarsen(newrows,newcols,FLL20.y);
FLL20y = FLL20y-110;
FLL20e1 = dataCoarsen(newrows,newcols,FLL20.e1);
FLL20e2 = dataCoarsen(newrows,newcols,FLL20.e2);
FLL20gamma = dataCoarsen(newrows,newcols,FLL20.gamma);
FLL20e1x = FLL20e1.*cos(FLL20gamma);
FLL20e1y = FLL20e1.*sin(FLL20gamma);
FLL20Pic = imread('FL12110306L Strain/FL12110306L-0243_0.tif');

% 0 DEG PA Cut
FLL30 = load('FL12110306L Strain/FL12110306L-0392_0 PACut 0DEG.mat');
FLL30x = dataCoarsen(newrows,newcols,FLL30.x);
FLL30y = dataCoarsen(newrows,newcols,FLL30.y);
FLL30y = FLL30y-80;
FLL30e1 = dataCoarsen(newrows,newcols,FLL30.e1);
FLL30e2 = dataCoarsen(newrows,newcols,FLL30.e2);
FLL30gamma = dataCoarsen(newrows,newcols,FLL30.gamma);
FLL30e1x = FLL30e1.*cos(FLL30gamma);
FLL30e1y = FLL30e1.*sin(FLL30gamma);
FLL30Pic = imread('FL12110306L Strain/FL12110306L-0392_0.tif');

%% MDL
% 0 DEG Intact
MDL00 = load('MD12101222L Strain Data/MD12101222L-0377_0 OG 0DEG.mat');
MDL00x = dataCoarsen(newrows,newcols,MDL00.x);
MDL00y = dataCoarsen(newrows,newcols,MDL00.y);
MDL00y = MDL00y-80;
MDL00e1 = dataCoarsen(newrows,newcols,MDL00.e1);
MDL00e2 = dataCoarsen(newrows,newcols,MDL00.e2);
MDL00gamma = dataCoarsen(newrows,newcols,MDL00.gamma);
MDL00e1x = MDL00e1.*cos(MDL00gamma);
MDL00e1y = MDL00e1.*sin(MDL00gamma);
MDL00Pic = imread('MD12101222L Strain Data/MD12101222L-0377_0.tif');

% 0 DEG P Cut
MDL20 = load('MD12101222L Strain Data/MD12101222L-0641_0 PCut 0DEG.mat');
MDL20x = dataCoarsen(newrows,newcols,MDL20.x);
MDL20y = dataCoarsen(newrows,newcols,MDL20.y);
MDL20y = MDL20y-80;
MDL20e1 = dataCoarsen(newrows,newcols,MDL20.e1);
MDL20e2 = dataCoarsen(newrows,newcols,MDL20.e2);
MDL20gamma = dataCoarsen(newrows,newcols,MDL20.gamma);
MDL20e1x = MDL20e1.*cos(MDL20gamma);
MDL20e1y = MDL20e1.*sin(MDL20gamma);
MDL20Pic = imread('MD12101222L Strain Data/MD12101222L-0641_0.tif');

% 0 DEG PA Cut
MDL30 = load('MD12101222L Strain Data/MD12101222L-1029_0 PACut 0DEG.mat');
MDL30x = dataCoarsen(newrows,newcols,MDL30.x);
MDL30y = dataCoarsen(newrows,newcols,MDL30.y);
MDL30y = MDL30y-80;
```

```
MDL30e1 = dataCoarsen(newrows,newcols,MDL30.e1);
MDL30e2 = dataCoarsen(newrows,newcols,MDL30.e2);
MDL30gamma = dataCoarsen(newrows,newcols,MDL30.gamma);
MDL30e1x = MDL30e1.*cos(MDL30gamma);
MDL30e1y = MDL30e1.*sin(MDL30gamma);
MDL30Pic = imread('MD12101222L Strain Data/MD12101222L-1029_0.tif');

%% TXL
% 0 DEG Intact
TXL00 = load('TX12091951L Strain Data/TX12091951L-0033 OG 0DEG.mat');
TXL00x = dataCoarsen(newrows,newcols,TXL00.x);
TXL00y = dataCoarsen(newrows,newcols,TXL00.y);
TXL00y = TXL00y-90;
TXL00e1 = dataCoarsen(newrows,newcols,TXL00.e1);
TXL00e2 = dataCoarsen(newrows,newcols,TXL00.e2);
TXL00gamma = dataCoarsen(newrows,newcols,TXL00.gamma);
TXL00e1x = TXL00e1.*cos(TXL00gamma);
TXL00e1y = TXL00e1.*sin(TXL00gamma);
TXL00Pic = imread('TX12091951L Strain Data/TX12091951L-0033_0.tif');

% 0 DEG P Cut
TXL20 = load('TX12091951L Strain Data/TX12091951L-0262 PCut 0DEG.mat');
TXL20x = dataCoarsen(newrows,newcols,TXL20.x);
TXL20y = dataCoarsen(newrows,newcols,TXL20.y);
TXL20y = TXL20y-80;
TXL20e1 = dataCoarsen(newrows,newcols,TXL20.e1);
TXL20e2 = dataCoarsen(newrows,newcols,TXL20.e2);
TXL20gamma = dataCoarsen(newrows,newcols,TXL20.gamma);
TXL20e1x = TXL20e1.*cos(TXL20gamma);
TXL20e1y = TXL20e1.*sin(TXL20gamma);
TXL20Pic = imread('TX12091951L Strain Data/TX12091951L-0262_0.tif');

% 0 DEG PA Cut
TXL30 = load('TX12091951L Strain Data/TX12091951L-0493 PACut 0DEG.mat');
TXL30x = dataCoarsen(newrows,newcols,TXL30.x);
TXL30y = dataCoarsen(newrows,newcols,TXL30.y);
TXL30y = TXL30y-80;
TXL30e1 = dataCoarsen(newrows,newcols,TXL30.e1);
TXL30e2 = dataCoarsen(newrows,newcols,TXL30.e2);
TXL30gamma = dataCoarsen(newrows,newcols,TXL30.gamma);
TXL30e1x = TXL30e1.*cos(TXL30gamma);
TXL30e1y = TXL30e1.*sin(TXL30gamma);
TXL30Pic = imread('TX12091951L Strain Data/TX12091951L-0493_0.tif');

%% TXR
% 0 DEG Intact
TXR00 = load('TX12091951R Strain Data/TX12091951-0086 OG 0DEG.mat');
TXR00x = dataCoarsen(newrows,newcols,TXR00.x);
TXR00x = TXR00x;
TXR00y = dataCoarsen(newrows,newcols,TXR00.y);
TXR00y = TXR00y - 200;
TXR00e1 = dataCoarsen(newrows,newcols,TXR00.e1);
TXR00e2 = dataCoarsen(newrows,newcols,TXR00.e2);
TXR00gamma = dataCoarsen(newrows,newcols,TXR00.gamma);
TXR00e1x = TXR00e1.*cos(TXR00gamma);
TXR00e1y = TXR00e1.*sin(TXR00gamma);
```

```
TXR00Pic = imread('TX12091951R Strain Data/TX12091951-0086_1.tif');

% 0 DEG P Cut
TXR20 = load('TX12091951R Strain Data/TX12091951-0238 PCut 0DEG.mat');
TXR20x = dataCoarsen(newrows,newcols,TXR20.x);
TXR20y = dataCoarsen(newrows,newcols,TXR20.y);
TXR20y = TXR20y - 200;
TXR20e1 = dataCoarsen(newrows,newcols,TXR20.e1);
TXR20e2 = dataCoarsen(newrows,newcols,TXR20.e2);
TXR20gamma = dataCoarsen(newrows,newcols,TXR20.gamma);
TXR20e1x = TXR20e1.*cos(TXR20gamma);
TXR20e1y = TXR20e1.*sin(TXR20gamma);
TXR20Pic = imread('TX12091951R Strain Data/TX12091951-0238_1.tif');

% 0 DEG PA Cut
TXR30 = load('TX12091951R Strain Data/TX12091951-0064 PACut 0DEG.mat');
TXR30x = dataCoarsen(newrows,newcols,TXR30.x);
TXR30x = TXR30x + 20;
TXR30y = dataCoarsen(newrows,newcols,TXR30.y);
TXR30y = TXR30y - 100;
TXR30e1 = dataCoarsen(newrows,newcols,TXR30.e1);
TXR30e2 = dataCoarsen(newrows,newcols,TXR30.e2);
TXR30gamma = dataCoarsen(newrows,newcols,TXR30.gamma);
TXR30e1x = TXR30e1.*cos(TXR30gamma);
TXR30e1y = TXR30e1.*sin(TXR30gamma);
TXR30Pic = imread('TX12091951R Strain Data/TX12091951-0064_1.tif');

%% VAR
% 0 DEG Intact
VAR00 = load('VA12100409R Strain Data/VA12100409R-0272 OG 0DEG.mat');
VAR00x = dataCoarsen(newrows,newcols,VAR00.x);
VAR00y = dataCoarsen(newrows,newcols,VAR00.y);
VAR00y = VAR00y-180;
VAR00e1 = dataCoarsen(newrows,newcols,VAR00.e1);
VAR00e2 = dataCoarsen(newrows,newcols,VAR00.e2);
VAR00gamma = dataCoarsen(newrows,newcols,VAR00.gamma);
VAR00e1x = VAR00e1.*cos(VAR00gamma);
VAR00e1y = VAR00e1.*sin(VAR00gamma);
VAR00Pic = imread('VA12100409R Strain Data/VA12100409R-0272_0.tif');

% 0 DEG P Cut
VAR20 = load('VA12100409R Strain Data/VA12100409R-0227 PCut 0DEG.mat');
VAR20x = dataCoarsen(newrows,newcols,VAR20.x);
VAR20x = VAR20x-50;
VAR20y = dataCoarsen(newrows,newcols,VAR20.y);
VAR20y = VAR20y-200;
VAR20e1 = dataCoarsen(newrows,newcols,VAR20.e1);
VAR20e2 = dataCoarsen(newrows,newcols,VAR20.e2);
VAR20gamma = dataCoarsen(newrows,newcols,VAR20.gamma);
VAR20e1x = VAR20e1.*cos(VAR20gamma);
VAR20e1y = VAR20e1.*sin(VAR20gamma);
VAR20Pic = imread('VA12100409R Strain Data/VA12100409R-0227_1.tif');

% 0 DEG PA Cut
VAR30 = load('VA12100409R Strain Data/VA12100409R-0571 PACut 0DEG.mat');
VAR30x = dataCoarsen(newrows,newcols,VAR30.x);
```

```
VAR30x = VAR30x - 117;
VAR30y = dataCoarsen(newrows,newcols,VAR30.y);
VAR30y = VAR30y-160;
VAR30e1 = dataCoarsen(newrows,newcols,VAR30.e1);
VAR30e2 = dataCoarsen(newrows,newcols,VAR30.e2);
VAR30gamma = dataCoarsen(newrows,newcols,VAR30.gamma);
VAR30e1x = VAR30e1.*cos(VAR30gamma);
VAR30e1y = VAR30e1.*sin(VAR30gamma);
VAR30Pic = imread('VA12100409R Strain Data/VA12100409R-0571_1.tif');


%%%%%%%%%% Plots %%%%%%%%%%
%% DEL
figure(),
imshow(DEL00Pic)
hold on
quiver(DEL00x,DEL00y,DEL00e1.*cos(DEL00gamma),DEL00e1.*sin(DEL00gamma),'LineW
idth',2,'AlignVertexCenters','on','Color',[1 1 0]);
title('DEL 0DEG Intact')
legend('E1');

figure(),
imshow(DEL10Pic)
hold on
quiver(DEL10x,DEL10y,DEL10e1.*cos(DEL10gamma),DEL10e1.*sin(DEL10gamma),'LineW
idth',2,'AlignVertexCenters','on','Color',[1 1 0]);
title('DEL 0DEG ACut')
legend('E1');

figure(),
imshow(DEL30Pic)
hold on
quiver(DEL30x,DEL30y,DEL30e1.*cos(DEL30gamma),DEL30e1.*sin(DEL30gamma),'LineW
idth',2,'AlignVertexCenters','on','Color',[1 1 0]);
title('DEL 0DEG APCut')
legend('E1');

%% FLL
figure(),
imshow(FLL00Pic)
hold on
quiver(FLL00x,FLL00y,FLL00e1.*cos(FLL00gamma),FLL00e1.*sin(FLL00gamma),'LineW
idth',2,'AlignVertexCenters','on','Color',[1 1 0]);
title('FLL 0DEG Intact')
legend('E1');

figure(),
imshow(FLL20Pic)
hold on
quiver(FLL20x,FLL20y,FLL20e1.*cos(FLL20gamma),FLL20e1.*sin(FLL20gamma),'LineW
idth',2,'AlignVertexCenters','on','Color',[1 1 0]);
title('FLL 0DEG PCut')
legend('E1');

figure(),
```

```
imshow(FLL30Pic)
hold on
quiver(FLL30x,FLL30y,FLL30e1.*cos(FLL30gamma),FLL30e1.*sin(FLL30gamma),'LineW
idth',2,'AlignVertexCenters','on','Color',[1 1 0]);
title('FLL 0DEG APCut')
legend('E1');

%% LAL
figure(),
imshow(LAL00Pic)
hold on
quiver(LAL00x,LAL00y,LAL00e1.*cos(LAL00gamma),LAL00e1.*sin(LAL00gamma),'LineW
idth',2,'AlignVertexCenters','on','Color',[1 1 0]);
title('LAL 0DEG Intact')
legend('E1');

figure(),
imshow(LAL10Pic)
hold on
quiver(LAL10x,LAL10y,LAL10e1.*cos(LAL10gamma),LAL10e1.*sin(LAL10gamma),'LineW
idth',2,'AlignVertexCenters','on','Color',[1 1 0]);
title('LAL 0DEG ACut')
legend('E1');

figure(),
imshow(LAL30Pic)
hold on
quiver(LAL30x,LAL30y,LAL30e1.*cos(LAL30gamma),LAL30e1.*sin(LAL30gamma),'LineW
idth',2,'AlignVertexCenters','on','Color',[1 1 0]);
title('LAL 0DEG APCut')
legend('E1');

%% LAR
figure(),
imshow(LAR00Pic)
hold on
quiver(LAR00x,LAR00y,LAR00e1.*cos(LAR00gamma),LAR00e1.*sin(LAR00gamma),'LineW
idth',2,'AlignVertexCenters','on','Color',[1 1 0]);
title('LAR 0DEG Intact')
legend('E1');

figure(),
imshow(LAR10Pic)
hold on
quiver(LAR10x,LAR10y,LAR10e1.*cos(LAR10gamma),LAR10e1.*sin(LAR10gamma),'LineW
idth',2,'AlignVertexCenters','on','Color',[1 1 0]);
title('LAR 0DEG ACut')
legend('E1');

figure(),
imshow(LAR30Pic)
hold on
quiver(LAR30x,LAR30y,LAR30e1.*cos(LAR30gamma),LAR30e1.*sin(LAR30gamma),'LineW
idth',2,'AlignVertexCenters','on','Color',[1 1 0]);
title('LAR 0DEG APCut')
legend('E1');
```

```
%
%% MDL
figure(),
imshow(MDL00Pic)
hold on
quiver(MDL00x,MDL00y,MDL00e1.*cos(MDL00gamma),MDL00e1.*sin(MDL00gamma),'LineW
idth',2,'AlignVertexCenters','on','Color',[1 1 0]);
title('MDL 0DEG Intact')
legend('E1');

figure(),
imshow(MDL20Pic)
hold on
quiver(MDL20x,MDL20y,MDL20e1.*cos(MDL20gamma),MDL20e1.*sin(MDL20gamma),'LineW
idth',2,'AlignVertexCenters','on','Color',[1 1 0]);
title('MDL 0DEG PCut')
legend('E1');

figure(),
imshow(MDL30Pic)
hold on
quiver(MDL30x,MDL30y,MDL30e1.*cos(MDL30gamma),MDL30e1.*sin(MDL30gamma),'LineW
idth',2,'AlignVertexCenters','on','Color',[1 1 0]);
title('MDL 0DEG APCut')
legend('E1');

%% MDR
figure(),
imshow(MDR00Pic)
hold on
quiver(MDR00x,MDR00y,MDR00e1.*cos(MDR00gamma),MDR00e1.*sin(MDR00gamma),'LineW
idth',2,'AlignVertexCenters','on','Color',[1 1 0]);
title('MDR 0DEG Intact')
legend('E1');

figure(),
imshow(MDR00Pic)
hold on
quiver(MDR00x,MDR00y,-1.*MDR00e1.*cos(MDR00gamma),-
1.*MDR00e1.*sin(MDR00gamma),'LineWidth',2,'AlignVertexCenters','on','Color',[
1 1 0]);
title('MDR 0DEG Intact')
legend('E1');

figure(),
imshow(MDR10Pic)
hold on
quiver(MDR10x,MDR10y,MDR10e1.*cos(MDR10gamma),MDR10e1.*sin(MDR10gamma),'LineW
idth',2,'AlignVertexCenters','on','Color',[1 1 0]);
title('MDR 0DEG ACut')
legend('E1');

figure(),
imshow(MDR30Pic)
hold on
```

```
quiver(MDR30x,MDR30y,MDR30e1.*cos(MDR30gamma),MDR30e1.*sin(MDR30gamma),'LineW
idth',2,'AlignVertexCenters','on','Color',[1 1 0]);
title('MDR 0DEG APCut')
legend('E1');

%% NCL
figure(),
imshow(NCL00Pic)
hold on
quiver(NCL00x,NCL00y,NCL00e1.*cos(NCL00gamma),NCL00e1.*sin(NCL00gamma),'LineW
idth',2,'AlignVertexCenters','on','Color',[1 1 0]);
title('NCL 0DEG Intact')
legend('E1');

figure(),
imshow(NCL10Pic)
hold on
quiver(NCL10x,NCL10y,NCL10e1.*cos(NCL10gamma),NCL10e1.*sin(NCL10gamma),'LineW
idth',2,'AlignVertexCenters','on','Color',[1 1 0]);
title('NCL 0DEG ACut')
legend('E1');

figure(),
imshow(NCL30Pic)
hold on
quiver(NCL30x,NCL30y,NCL30e1.*cos(NCL30gamma),NCL30e1.*sin(NCL30gamma),'LineW
idth',2,'AlignVertexCenters','on','Color',[1 1 0]);
title('NCL 0DEG APCut')
legend('E1');

%% TXL
figure(),
imshow(TXL00Pic)
hold on
quiver(TXL00x,TXL00y,TXL00e1.*cos(TXL00gamma),TXL00e1.*sin(TXL00gamma),'LineW
idth',2,'AlignVertexCenters','on','Color',[1 1 0]);
title('TXL 0DEG Intact')
legend('E1');

figure(),
imshow(TXL20Pic)
hold on
quiver(TXL20x,TXL20y,TXL20e1.*cos(TXL20gamma),TXL20e1.*sin(TXL20gamma),'LineW
idth',2,'AlignVertexCenters','on','Color',[1 1 0]);
title('TXL 0DEG PCut')
legend('E1');

figure(),
imshow(TXL30Pic)
hold on
quiver(TXL30x,TXL30y,TXL30e1.*cos(TXL30gamma),TXL30e1.*sin(TXL30gamma),'LineW
idth',2,'AlignVertexCenters','on','Color',[1 1 0]);
title('TXL 0DEG APCut')
legend('E1');
%
%% TXR
```

```
figure(),
imshow(TXR00Pic)
hold on
quiver(TXR00x,TXR00y,TXR00e1.*cos(TXR00gamma),TXR00e1.*sin(TXR00gamma),'LineW
idth',2,'AlignVertexCenters','on','Color',[1 1 0]);
title('TXR 0DEG Intact')
legend('E1');

figure(),
imshow(TXR20Pic)
hold on
quiver(TXR20x,TXR20y,TXR20e1.*cos(TXR20gamma),TXR20e1.*sin(TXR20gamma),'LineW
idth',2,'AlignVertexCenters','on','Color',[1 1 0]);
title('TXR 0DEG PCut')
legend('E1');

figure(),
imshow(TXR30Pic)
hold on
quiver(TXR30x,TXR30y,TXR30e1.*cos(TXR30gamma),TXR30e1.*sin(TXR30gamma),'LineW
idth',2,'AlignVertexCenters','on','Color',[1 1 0]);
title('TXR 0DEG APCut')
legend('E1');

%% VAR
figure(),
imshow(VAR00Pic)
hold on
quiver(VAR00x,VAR00y,VAR00e1.*cos(VAR00gamma),VAR00e1.*sin(VAR00gamma),'LineW
idth',2,'AlignVertexCenters','on','Color',[1 1 0]);
title('VAR 0DEG Intact')
legend('E1');

figure(),
imshow(VAR20Pic)
hold on
quiver(VAR20x,VAR20y,VAR20e1.*cos(VAR20gamma),VAR20e1.*sin(VAR20gamma),'LineW
idth',2,'AlignVertexCenters','on','Color',[1 1 0]);
title('VAR 0DEG PCut')
legend('E1');

figure(),
imshow(VAR30Pic)
hold on
quiver(VAR30x,VAR30y,VAR30e1.*cos(VAR30gamma),VAR30e1.*sin(VAR30gamma),'LineW
idth',2,'AlignVertexCenters','on','Color',[1 1 0]);
title('VAR 0DEG APCut')
legend('E1');
```

A.2 Average Data Matlab Code

```
function [datacoarse] = dataCoarsen(inputrow, inputcol,data)
%% Average/Coarsen Matrix

% Written by Sean Delserro
% Graduate Research Assistant
% Shoulder and Elbow Mechanics Laboratory
% May 29, 2018


% This code averages the data output from the DIC into a distinct
% number of regions.  The end result is a 2-D matrix defined by the
% number of zones input by the user

newrows = inputrow;
newcols = inputcol;

[oldrows,oldcols] = size(data);

%This defines average box size
inputrowratio = round(oldrows/newrows);
inputcolratio = round(oldcols/newcols);
rowratio = inputrowratio;
colratio = inputcolratio;
datacoarse = zeros(newrows,newcols);

for i = 1:newrows

    for j = 1:newcols
        colaverage=0;

        %Checks to see if average box iteration exceeds dimensions of
        %original matrix

        if j*colratio > oldcols
                colratio = colratio - (j*colratio-oldcols);
        end
        temp = zeros(1,colratio);

        for m = 1:colratio
            rowaverage=0;

            %Checks to see if average box iteration exceeds dimensions of
            %original matrix

                if i*rowratio > oldrows
                        rowratio = rowratio-(i*rowratio-oldrows);
                end

                for k = 1:rowratio
```

```
                    tempx = (i-1)*inputrowratio+k;
                    if tempx > oldrows
                        rowaverage=NaN;
                    else
                        rowaverage = rowaverage + data(tempx,(j-
1)*inputcolratio+m);

                    end
                end
            temp(1,m) = rowaverage/rowratio;
            colaverage = colaverage + temp(1,m);
        end
        datacoarse(i,j) = colaverage/colratio;
    end
end
end
```

Appendix B Major Principal Strain and Strain Angle Data

Table 3. Major Principal Strain vs. Zone at 0 Degrees Abduction (Anterior Group, *, p<0.05)**

Zones (0 DEG)	Intact	Anterior Release	Full Release
1	0.046 ± .0032	0.002 ± 0.002	0.001 ± 0.001
2	0.020 ± 0.007*	0.009 ± 0.007	0.005 ± 0.006*
3	0.018 ± 0.011	0.020 ± 0.014	0.015 ± 0.008
4	0.014 ± 0.008	0.020 ± 0.012	0.014 ± 0.010
5	0.006 ± 0.007	0.003 ± 0.004	0.005 ± 0.004
6	0.013 ± 0.006	0.011 ± 0.003	0.010 ± 0.005
7	0.016 ± 0.008	0.017 ± 0.012	0.016 ± 0.008
8	0.018 ± 0.013	0.022 ± 0.016	0.020 ± 0.009
9	0.021 ± 0.012	0.021 ± 0.008	0.022 ± 0.008
10	0.016 ± 0.006	0.017 ± 0.007	0.021 ± 0.012
11	0.013 ± 0.009	0.014 ± 0.006	0.008 ± 0.004
12	0.017 ± 0.004	0.019 ± 0.007	0.014 ± 0.006
13	0.017 ± 0.006	0.019 ± 0.009	0.016 ± 0.005
14	0.016 ± 0.005	0.021 ± 0.011	0.018 ± 0.004
15	0.015 ± 0.005	0.016 ± 0.006	0.017 ± 0.017
16	0.002 ± 0.002	0.002 ± 0.001	0.002 ± 0.001
17	0.012 ± 0.004	0.014 ± 0.007	0.012 ± 0.003
18	0.016 ± 0.009	0.015 ± 0.006	0.016 ± 0.004
19	0.015 ± 0.004	0.015 ± 0.004	0.013 ± 0.006
20	0.004 ± 0.002	0.003 ± 0.002	0.003 ± 0.003

Table 4. Major Principal Strain vs. Zone at 45 Degrees Abduction (Anterior Group, *, p<0.05)**

Zones (45 DEG)	Intact	Anterior Release	Full Release
1	0.002 ± 0.003	0.005 ± 0.008	0.002 ± 0.003
2	0.021 ± 0.026	0.015 ± 0.024	0.010 ± 0.008
3	0.028 ± 0.030	0.016 ± 0.019	0.017 ± 0.012
4	0.020 ± 0.020	0.010 ± 0.010	0.008 ± 0.006
5	0.004 ± 0.004	0.002 ± 0.003	0.002 ± 0.001
6	0.017 ± 0.010	0.015 ± 0.013	0.012 ± 0.012
7	0.021 ± 0.020	0.017 ± 0.014	0.014 ± 0.008
8	0.017 ± 0.019	0.018 ± 0.013	0.015 ± 0.009
9	0.016 ± 0.016	0.021 ± 0.014	0.017 ± 0.008
10	0.015 ± 0.014	0.014 ± 0.007	0.013 ± 0.007
11	0.014 ± 0.005	0.008 ± 0.004	0.009 ± 0.004
12	0.010 ± 0.003	0.012 ± 0.003	0.011 ± 0.003
13	0.011 ± 0.005	0.014 ± 0.004	0.013 ± 0.003
14	0.012 ± 0.001	0.018 ± 0.004	0.016 ± 0.004
15	0.016 ± 0.007	0.017 ± 0.008	0.013 ± 0.005
16	0.002 ± 0.002	0.002 ± 0.002	0.001 ± 0.001
17	0.006 ± 0.004	0.007 ± 0.005	0.007 ± 0.003
18	0.006 ± 0.006	0.008 ± 0.006	0.009 ± 0.004
19	0.008 ± 0.004	0.014 ± 0.005	0.010 ± 0.006
20	0.005 ± 0.003	0.008 ± 0.008	0.006 ± 0.006

Table 5. Major Principal Strain vs. Zone at 90 Degrees Abduction (Anterior Group, *, p<0.05)**

Zones (90 DEG)	Intact	Anterior Release	Full Release
1	0.001 ± 0.002	0.001 ± 0.002	0.001 ± 0.001
2	0.007 ± 0.007	0.013 ± 0.016	0.016 ± 0.019
3	0.012 ± 0.015	0.016 ± 0.019	0.020 ± 0.018
4	0.014 ± 0.017	0.008 ± 0.013	0.010 ± 0.012
5	0.003 ± 0.004	0.001 ± 0.002	0.004 ± 0.007
6	0.013 ± 0.011	0.013 ± 0.020	0.012 ± 0.012
7	0.025 ± 0.013	0.033 ± 0.034	0.028 ± 0.020
8	0.036 ± 0.020	0.039 ± 0.030	0.037 ± 0.026
9	0.041 ± 0.025	0.029 ± 0.027	0.033 ± 0.020
10	0.026 ± 0.019	0.016 ± 0.008	0.015 ± 0.006
11	0.020 ± 0.017	0.022 ± 0.037	0.016 ± 0.013
12	0.017 ± 0.008	0.017 ± 0.010	0.015 ± 0.012
13	0.024 ± 0.017	0.025 ± 0.023	0.022 ± 0.020
14	0.029 ± 0.014	0.033 ± 0.021	0.028 ± 0.019
15	0.020 ± 0.010	0.025 ± 0.017	0.018 ± 0.008
16	0.004 ± 0.003	0.004 ± 0.004	0.005 ± 0.004
17	0.006 ± 0.003	0.006 ± 0.005	0.010 ± 0.008
18	0.005 ± 0.004	0.007 ± 0.008	0.008 ± 0.007
19	0.010 ± 0.007	0.015 ± 0.011	0.010 ± 0.009
20	0.009 ± 0.009	0.017 ± 0.017	0.009 ± 0.009

Table 6. Major Principal Strain vs. Zone at 0 Degrees Abduction (Posterior Group, *, p<0.05)**

Zones (0 DEG)	Intact	Posterior Release	Full Release
1	0.005 ± 0.004	0.009 ± 0.008	0.007 ± 0.010
2	0.012 ± 0.011	0.022 ± 0.012	0.019 ± 0.012
3	0.021 ± 0.013	0.030 ± 0.020	0.026 ± 0.025
4	0.025 ± 0.015	0.029 ± 0.020	0.025 ± 0.021
5	0.013 ± 0.007	0.009 ± 0.005	0.006 ± 0.006
6	0.013 ± 0.009	0.029 ± 0.006	0.018 ± 0.008
7	0.018 ± 0.009	0.030 ± 0.015	0.029 ± 0.016
8	0.028 ± 0.012	0.033 ± 0.017	0.034 ± 0.019
9	0.034 ± 0.014	0.034 ± 0.017	0.041 ± 0.019
10	0.035 ± 0.013	0.027 ± 0.008	0.027 ± 0.011
11	0.013 ± 0.009	0.020 ± 0.006	0.016 ± 0.007
12	0.022 ± 0.009	0.019 ± 0.012	0.023 ± 0.007
13	0.028 ± 0.011	0.024 ± 0.010	0.026 ± 0.011
14	0.030 ± 0.014	0.032 ± 0.019	0.038 ± 0.023
15	0.021 ± 0.006	0.029 ± 0.017	0.029 ± 0.018
16	0.002 ± 0.002	0.003 ± 0.002	0.002 ± 0.001
17	0.011 ± 0.004	0.015 ± 0.007	0.018 ± 0.009
18	0.017 ± 0.004	0.017 ± 0.003	0.018 ± 0.011
19	0.019 ± 0.006	0.018 ± 0.009	0.016 ± 0.009
20	0.006 ± 0.003	0.007 ± 0.008	0.007 ± 0.004

Table 7. Major Principal Strain vs. Zone at 45 Degrees Abduction (Posterior Group, *, p<0.05)**

Zones (45 DEG)	Intact	Posterior Release	Full Release
1	0.001 ± 0.001	0.005 ± 0.006	0.004 ± 0.005
2	0.006 ± 0.007	0.017 ± 0.014	0.014 ± 0.014
3	0.013 ± 0.013	0.024 ± 0.016	0.029 ± 0.014
4	0.018 ± 0.017	0.023 ± 0.008	0.019 ± 0.010
5	0.006 ± 0.005	0.005 ± 0.004	0.004 ± 0.004
6	0.015 ± 0.023	0.023 ± 0.015	0.019 ± 0.010
7	0.011 ± 0.014	0.022 ± 0.010	0.023 ± 0.009
8	0.020 ± 0.024	0.027 ± 0.017	0.023 ± 0.015
9	0.032 ± 0.039	0.032 ± 0.017	0.024 ± 0.013
10	0.020 ± 0.012	0.024 ± 0.009	0.022 ± 0.016
11	0.014 ± 0.018	0.023 ± 0.015	0.011 ± 0.004
12	0.015 ± 0.012	0.022 ± 0.012	0.015 ± 0.006
13	0.014 ± 0.007	0.020 ± 0.008	0.019 ± 0.007
14	0.022 ± 0.016	0.027 ± 0.012	0.021 ± 0.014
15	0.024 ± 0.016	0.028 ± 0.012	0.028 ± 0.021
16	0.004 ± 0.005	0.006 ± 0.004	0.001 ± 0.001
17	0.009 ± 0.008	0.012 ± 0.009	0.008 ± 0.005
18	0.008 ± 0.004	0.023 ± 0.018	0.012 ± 0.005
19	0.011 ± 0.010	0.031 ± 0.042	0.018 ± 0.011
20	0.004 ± 0.004	0.014 ± 0.013	0.006 ± 0.003

Table 8. Major Principal Strain vs. Zone at 90 Degrees Abduction (Posterior Group, *, p<0.05)**

Zones (90 DEG)	Intact	Posterior Release	Full Release
1	0.005 ± 0.005	0.008 ± 0.009	0.000 ± 0.001
2	0.018 ± 0.016	0.027 ± 0.018	0.018 ± 0.017
3	0.009 ± 0.032	0.129 ± 0.234	0.026 ± 0.033
4	0.010 ± 0.026	0.170 ± 0.340	0.017 ± 0.020
5	0.014 ± 0.019	0.053 ± 0.113	0.006 ± 0.007
6	0.027 ± 0.014	0.181 ± 0.347	0.007 ± 0.004
7	0.030 ± 0.020	0.171 ± 0.325	0.020 ± 0.014
8	0.019 ± 0.013	0.035 ± 0.042	0.024 ± 0.022
9	0.023 ± 0.014	-0.096 ± 0.270	0.030 ± 0.030
10	0.032 ± 0.020	-0.184 ± 0.473	0.032 ± 0.037
11	0.015 ± 0.008	0.154 ± 0.317	0.014 ± 0.012
12	0.017 ± 0.011	0.101 ± 0.201	0.014 ± 0.010
13	0.014 ± 0.008	-0.138 ± 0.345	0.017 ± 0.015
14	0.017 ± 0.010	-0.150 ± 0.400	0.028 ± 0.033
15	0.029 ± 0.017	-0.174 ± 0.470	0.030 ± 0.040
16	0.003 ± 0.001	0.000 ± 0.008	0.002 ± 0.001
17	0.008 ± 0.004	-0.008 ± 0.036	0.006 ± 0.004
18	0.007 ± 0.002	-0.032 ± 0.099	0.012 ± 0.008
19	0.007 ± 0.007	-0.064 ± 0.187	0.014 ± 0.011
20	0.006 ± 0.006	-0.047 ± 0.118	0.007 ± 0.005

Table 9. Strain Angle (Radians) vs. Zone at 0 Degrees Abduction (Anterior Group, *· p<0.05)**

Zones (0 DEG)	Intact	Anterior Release	Full Release
1	-0.126 ± 0.258	0.005 ± 0.090	-0.034 ± 0.084
2	-0.380 ± 0.809	-0.175 ± 0.399	-0.094 ± 0.530
3	-0.585 ± 0.384	0.044 ± 0.791	-0.020 ± 0.592
4	0.134 ± 0.689	0.151 ± 0.518	0.002 ± 0.418
5	0.258 ± 0.218	0.130 ± 0.173	0.096 ± 0.218
6	-0.351 ± 0.699	0.224 ± 0.451	-0.216 ± 0.537
7	-0.786 ± 0.924	0.037 ± 0.851	0.134 ± 1.237
8	-0.535 ± 0.766	-0.050 ± 1.234	-0.062 ± 1.242
9	0.288 ± 1.294	0.211 ± 0.973	0.148 ± 0.972
10	0.191 ± 0.740	0.604 ± 0.410	0.288 ± 0.512
11	-0.163 ± 0.568	0.171 ± 0.469	-0.177 ± 0.386
12	-0.211 ± 1.289	-0.110 ± 1.038	0.478 ± 1.095
13	-0.617 ± 1.109	0.113 ± 1.273	0.184 ± 1.064
14	0.078 ± 1.254	0.088 ± 1.260	-0.121 ± 0.963
15	0.189 ± 0.740	0.348 ± 0.423	-0.101 ± 0.390
16	-0.024 ± 0.149	-0.046 ± 0.087	0.040 ± 0.082
17	-0.072 ± 0.844	0.020 ± 0.869	0.573 ± 0.744
18	-0.075 ± 1.154	-0.050 ± 0.843	0.251 ± 0.885
19	0.038 ± 0.598	-0.118 ± 0.923	-0.259 ± 0.723
20	0.179 ± 0.252	-0.102 ± 0.164	-0.025 ± 0.109

Table 10. Strain Angle (Radians) vs. Zone at 45 Degrees Abduction (Anterior Group, *· p<0.05)**

Zones (45 DEG)	Intact	Anterior Release	Full Release
1	0.043 ± 0.051	0.121 ± 0.285	-0.045 ± 0.103
2	0.190 ± 0.641	0.186 ± 0.784	-0.212 ± 0.630
3	-0.034 ± 1.084	-0.050 ± 0.856	0.022 ± 1.030
4	0.376 ± 0.424	0.120 ± 0.504	0.147 ± 0.550
5	0.187 ± 0.132	0.094 ± 0153	0.075 ± 0.165
6	0.327 ± 0.720	0.207 ± 0.515	-0.048 ± 0.482
7	0.504 ± 0.873	-0.198 ± 1.078	-0.181 ± 1.058
8	-0.061 ± 1.571	-0.198 ± 1.308	0.061 ± 1.330
9	0.913 ± 0.665	0.466 ± 1.077	0.219 ± 1.025
10	0.870 ± 0.322	0.175 ± 0.500	0.260 ± 0.673
11	0.252 ± 0.730	-0.128 ± 0.712	-0.570 ± 0.438
12	0.056 ± 1.115	-0.596 ± 1.051	-0.234 ± 1.256
13	-0.501 ± 1.247	-0.775 ± 1.034	-0.470 ± 0.959
14	0.248 ± 0.788	-0.489 ± 1.055	-0.191 ± 1.089
15	0.864 ± 0.455	0.014 ± 1.026	0.150 ± 1.017
16	0.093 ± 0.090	0.047 ± 0.151	-0.129 ± 0.117
17	0.029 ± 0.728	0.079 ± 0.818	-0.130 ± 0.774
18	0.073 ± 0.853	-0.159 ± 0.642	-0.279 ± 0.919
19	0.651 ± 0.287	-0.250 ± 0.793	-0.058 ± 0.663
20	0.387 ± 0.175	0.017 ± 0.599	0.061 ± 0.453

Table 11. Strain Angle (Radians) vs. Zone at 90 Degrees Abduction (Anterior Group, *· p<0.05)**

Zones (90 DEG)	Intact	Anterior Release	Full Release
1	0.071 ± 0.157	-0.048 ± 0.086	-0.025 ± 0.047
2	-0.038 ± 0.806	0.098 ± 0.577	0.166 ± 0.590
3	0.136 ± 0.581	-0.200 ± 0.684	0.353 ± 0.910
4	0.140 ± 0.666	0.429 ± 0.413	0.684 ± 0.185
5	-0.009 ± 0.168	0.020 ± 0.155	0.103 ± 0.176
6	-0.154 ± 0.292	0.183 ± 0.415	0.147 ± 0.318
7	-0.067 ± 1.171	0.106 ± 0.925	0.196 ± 0.892
8	0.480 ± 1.023	-0.308 ± 1.348	-0.134 ± 1.280
9	0.533 ± 0.851	0.225 ± 0.713	0.683 ± 0.699
10	-0.034 ± 0.924	0.132 ± 0.717	0.331 ± 0.379
11	-0.438 ± 0.737	0.206 ± 0.652	0.411 ± 0.626
12	-0.604 ± 0.663	-0.160 ± 0.911	0.145 ± 0.865
13	0.088 ± 0.942	-0.331 ± 0.964	0.176 ± 1.048
14	0.495 ± 0.829	0.206 ± 1.102	0.850 ± 0.672
15	0.293 ± 0.875	0.118 ± 0.820	0.405 ± 0.551
16	-0.054 ± 0.353	0.092 ± 0.296	0.174 ± 0.190
17	-0.248 ± 0.749	0.018 ± 0.617	0.102 ± 0.854
18	0.306 ± 0.551	0.062 ± 0.557	0.373 ± 0.526
19	0.297 ± 0.750	0.545 ± 0.355	0.287 ± 0.629
20	0.038 ± 0.417	0.153 ± 0.196	0.019 ± 0.546

Table 12. Strain Angle (Radians) vs. Zone at 0 Degrees Abduction (Posterior Group, *, p<0.05)**

Zones (0 DEG)	Intact	Posterior Release	Full Release
1	-0.003 ± 0.203	0.092 ± 0.092	0.129 ± 0.320
2	0.237 ± 0.654	0.413 ± 0.421	-0.004 ± 0.699
3	-0.173 ± 0.703	-0.043 ± 1.054	-0.018 ± 0.695
4	-0.465 ± 0.577	-0.063 ± 0.814	0.028 ± 0.364
5	0.027 ± 0.332	0.131 ± 0.142	0.005 ± 0.037
6	-0.065 ± 0.220	0.458 ± 0.367	0.310 ± 0.359
7	0.430 ± 0.496	0.745 ± 0.704	-0.425 ± 1.109
8	0.124 ± 1.195	0.187 ± 1.223	0.180 ± 1.205
9	-0.368 ± 1.006	0.135 ± 0.946	0.059 ± 0.809
10	0.069 ± 0.745	0.337 ± 0.401	0.000 ± 0.320
11	0.085 ± 0.239	0.134 ± 0.536	-0.194 ± 0.416
12	0.496 ± 1.004	0.453 ± 0.571	-0.393 ± 1.007
13	0.238 ± 1.078	-0.113 ± 0.879	-0.059 ± 0.937
14	-0.220 ± 0.959	-0.118 ± 0.787	-0.173 ± 0.636
15	0.265 ± 0.453	0.293 ± 0.534	0.048 ± 0.328
16	-0.051 ± 0.183	0.022 ± 0.078	0.002 ± 0.060
17	0.028 ± 0.349	0.186 ± 0.526	-0.151 ± 0.627
18	-0.551 ± 0.450	-0.577 ± 0.470	-0.195 ± 0.709
19	-0.623 ± 0.624	-0.040 ± 0.505	0.022 ± 0.272
20	-0.069 ± 0.228	0.091 ± 0.293	0.003 ± 0.284

Table 13. Strain Angle (Radians) vs. Zone at 45 Degrees Abduction (Posterior Group, *, p<0.05)**

Zones (45 DEG)	Intact	Posterior Release	Full Release
1	0.083 ± 0.128	0.215 ± 0.185	0.113 ± 0.136
2	-0.172 ± 0.563	0.289 ± 0.822	0.428 ± 0.546
3	-0.271 ± 0.953	0.216 ± 0.821	-0.186 ± 0.907
4	-0.090 ± 0.717	0.083 ± 0.782	0.224 ± 0.677
5	0.212 ± 0.174	-0.088 ± 0.169	0.078 ± 0.157
6	0.186 ± 0.646	0.521 ± 0.416	0.359 ± 0.513
7	0.259 ± 0.434	0.641 ± 0.386	0.044 ± 1.039
.1	0.281 ± 1.085	0.211 ± 1.291	-0.152 ± 1.099
9	0.413 ± 1.198	0.197 ± 1.071	0.013 ± 0.979
10	0.422 ± 0.901	-0.147 ± 0.601	0.586 ± 0.597
11	0.066 ± 0.586	-0.147 ± 0.568	-0.121 ± 0.683
12	0.669 ± 0.420	0.466 ± 0.814	-0.162 ± 0.565
13	0.479 ± 1.070	0.231 ± 0.910	0.042 ± 0.931
14	0.174 ± 1.391	-0.559 ± 0.960	-0.102 ± 0.888
15	-0.050 ± 0.927	-0.659 ± 0.483	0.359 ± 0.673
16	0.159 ± 0.304*,**	-0.047 ± 0.174*	0.035 ± 0.047**
17	0.247 ± 0.656	-0.238 ± 0.340	0.033 ± 0.730
18	0.160 ± 0.754	-0.611 ± 0.367	-0.436 ± 0.847
19	-0.158 ± 0.462	-0.395 ± 0.416	-0.294 ± 0.588
20	-0.035 ± 0.151	-0.021 ± 0.489	-0.002 ± 0.216

Table 14. Strain Angle (Radians) vs. Zone at 90 Degrees Abduction (Posterior Group, *, p<0.05)**

Zones (90 DEG)	Intact	Posterior Release	Full Release
1	0.009 ± 0.122	0.030 ± 0.142	-0.024 ± 0.060
2	-0.086 ± 0.671	0.159 ± 0.462	-0.260 ± 0.397
3	-0.258 ± 0.689	0.511 ± 0.580	0.044 ± 0.791
4	0.007 ± 0.687	0.564 ± 0.332	-0.023 ± 0.623
5	0.030 ± 0.411	0.064 ± 0.119	0.027 ± 0.195
6	0.339 ± 0.600	0.138 ± 0.763	-0.377 ± 0.394
7	-0.190 ± 0.956	-0.044 ± 0.805	0.097 ± 0.862
8	-0.193 ± 0.970	0.390 ± 0.371	-0.038 ± 0.513
9	-0.352 ± 1.126	0.569 ± 0.719	-0.197 ± 0.988
10	-0.370 ± 1.074	0.223 ± 0.750	0.082 ± 0.691
11	0.339 ± 0.755	0.116 ± 0.695	-0.390 ± 0.601
12	-0.087 ± 1.029	0.281 ± 0.387	-0.013 ± 0.440
13	0.211 ± 0.906	0.322 ± 0.821	-0.278 ± -0.888
14	0.013 ± 1.064	0.161 ± 0.744	-0.347 ± 0.817
15	0.058 ± 0.863	-0.054 ± 0.753	-0.025 ± 0.693
16	-0.040 ± 0.300	0.051 ± 0.320	-0.065 ± 0.169
17	-0.243 ± 0.680	0.268 ± 0.539	-0.041 ± 0.482
18	0.000 ± 0.417	0.391 ± 0.589	-0.050 ± 0.625
19	0.018 ± 0.373	-0.177 ± 0.485	0.035 ± 0.672
20	0.240 ± 0.470	-0.026 ± 0.182	0.056 ± 0.357

Table 15. Major Principal Strain Combined Group at 0° Abduction, Zones 18 & 19

Zones (0 DEG)	Intact	Full Release
18	0.016 ± 0.001	0.017 ± 0.002
19	0.017 ± 0.003	0.015 ± 0.002

Table 16. Major Principal Strain Combined Group at 45° Abduction, Zones 18 & 19

Zones (45 DEG)	Intact	Full Release
18	0.007 ± 0.001	0.011 ± 0.002
19	0.010 ± 0.002	0.014 ± 0.005

Table 17. Major Principal Strain Combined Group at 90° Abduction, Zones 18 & 19

Zones (90 DEG)	Intact	Full Release
18	0.006 ± 0.001	0.010 ± 0.003
19	0.008 ± 0.003	0.012 ± 0.003

Table 18. Strain Angle (Radians) Combined Group at 0° Abduction, Zones 18 & 19

Zones (0 DEG)	Intact	Full Release
18	-0.313 ± 0.863	0.028 ± 0.792
19	-0.292 ± 0.673	-0.118 ± 0.536

Table 19. Strain Angle (Radians) Combined Group at 45° Abduction, Zones 18 & 19

Zones (45 DEG)	Intact	Full Release
18	0.122 ± 0.748	-0.305 ± 0.871
19	0.201 ± 0.565	-0.143 ± 0.631

Table 20. Strain Angle (Radians) Combined Group at 90° Abduction, Zones 18 & 19

Zones (90 DEG)	Intact	Full Release
18	0.153 ± 0.488	0.161 ± 0.588
19	0.157 ± 0.577	0.161 ± 0.628

Bibliography

1. Kim, MD, H. Mike, et al. "Location and Initiation of Degenerative Rotator Cuff Tears."*Journal of Bone and Joint Surgery* (2010): 1088-1096.

2. Burkhart, SS. "Arthroscopic treatment of massive rotator cuff tears. Clinical results and biomechanical rationale." *Clinical Orthopaedics and Related Research* 267 (1991): 45-56.

3. Burkhart, SS. "Fluoroscopic comparison of kinematic patterns in massive rotator cuff tears: a suspension bridge model." *Clinical Orthopaedics and Related Research* 284 (1992): 144-152.

4. Gray, H., *Anatomy of the Human Body.* 20th ed. 1918. Philadelphia: Lea and Febiger.

5. Clark, J. M. "Tendons, ligaments, and capsule of the rotator cuff. Gross and microscopic anatomy." *The Journal of bone and joint surgery. American volume* 74.5 (1992): 713-725.

6. Mihata, Teruhisa, et al. "Clinical results of arthroscopic superior capsule reconstruction for irreparable rotator cuff tears." *Arthroscopy: The Journal of Arthroscopic & Related Surgery* 29.3 (2013): 459-470.

7. Ishihara, Yoko, et al. "Role of the superior shoulder capsule in passive stability of the glenohumeral joint." *Journal of shoulder and elbow surgery* 23.5 (2014): 642-648.

8. Inman, Verne T., and LeRoy C. Abbott. "Observations on the function of the shoulder joint." *JBJS* 26.1 (1944): 1-30.

9. Renström P, Arms SW, Stanwyck TS, Johnson RJ, Pope MH (1986) Strain within the anterior cruciate ligament during hamstring and quadriceps activity*. Am J Sports Med SAGE Publications 14:83–87

10. Reilly, P., Amis, A. A., Wallace, A. L., & Emery, R. J. H. (2003). Mechanical factors in the initiation and propagation of tears of the rotator cuff: quantification of strains o the supraspinatus tendon in vitro. *The Journal of bone and joint surgery. British volume, 85*(4), 594-599.

11. Mazzocca, A. D., Rincon, L. M., O'Connor, R. W., Obopilwe, E., Andersen, M., Geaney, L., & Arciero, R. A. (2008). Intra-articular partial-thickness rotator cuff tears: analysis of injured and repaired strain behavior. *The American journal of sports medicine,* 36(1), 110-116.

12. Andarawis-Puri, N, Ricchetti, E. T., & Soslowsky, L. J. (2009). Rotator cuff tendon strain correlates with tear propagation. *Journal of Biomechanics,* 42(2), 158-163.